Anal Bioanal Chem (2004) 378 : 256–269
DOI 10.1007/s00216-003-2233-2

ORIGINAL PAPER

Jan Kaiser · Sunyoung Park · Kristie A. Boering
Carl A. M. Brenninkmeijer · Andreas Hilkert
Thomas Röckmann

Mass spectrometric method for the absolute calibration of the intramolecular nitrogen isotope distribution in nitrous oxide

Received: 17 June 2003 / Revised: 11 August 2003 / Accepted: 13 August 2003 / Published online: 16 October 2003

Abstract A mass spectrometric method to determine the absolute intramolecular (position-dependent) nitrogen isotope ratios of nitrous oxide (N_2O) has been developed. It is based on the addition of different amounts of doubly labeled $^{15}N_2O$ to an N_2O sample of the isotope ratio mass spectrometer reference gas, and subsequent measurement of the relative ion current ratios of species with mass 30, 31, 44, 45, and 46. All relevant quantities are measured by isotope ratio mass spectrometers, which means that the machines' inherent high precision of the order of 10^{-5} can be fully exploited. External determination of dilution factors with generally lower precision is avoided. The method itself can be implemented within a day, but a calibration of the oxygen and average nitrogen isotope ratios relative to a primary isotopic reference material of known absolute isotopic composition has to be performed separately. The underlying theoretical framework is explored in depth. The effect of interferences due to $^{14}N^{15}N^{16}O$ and $^{15}N^{14}N^{16}O$ in the $^{15}N_2O$ sample and due to $^{15}N_2^+$ formation are fully accounted for in the calculation of the final position-dependent nitrogen isotope ratios. Considering all known statistical uncertainties of measured quantities and absolute isotope ratios of primary isotopic reference materials, we achieve an overall uncertainty of 0.9‰ (1σ). Using tropospheric N_2O as common reference point for intercomparison purposes, we find a substantially higher relative enrichment of ^{15}N at the central nitrogen atom over ^{15}N at the terminal nitrogen atom than measured previously for tropospheric N_2O based on a chemical conversion method: 46.3±1.4‰ as opposed to 18.7±2.2‰. However, our method depends critically on the absolute isotope ratios of the primary isotopic reference materials air–N_2 and VSMOW. If they are systematically wrong, our estimates will also necessarily be incorrect.

Keywords Nitrous oxide · Isotopic composition · Absolute position-dependent calibration · Intramolecular nitrogen isotope ratios · Isotope ratio mass spectrometry

J. Kaiser (✉) · C. A. M. Brenninkmeijer
Department of Atmospheric Chemistry,
Max Planck Institute for Chemistry, Mainz, Germany
e-mail: kaiser@princeton.edu

J. Kaiser · T. Röckmann
Atmospheric Physics Division,
Max Planck Institute for Nuclear Physics, Heidelberg, Germany

S. Park · K. A. Boering
Department of Earth and Planetary Science,
University of California, Berkeley, California, USA

K. A. Boering
Department of Chemistry, University of California,
Berkeley and Earth Science Division,
Lawrence Berkeley National Laboratory,
Berkeley, California, USA

A. Hilkert
Thermo Finnigan MAT, Bremen, Germany

Present address:
J. Kaiser
Department of Geosciences, Princeton University,
Washington Road, Princeton, New Jersey 08544, USA

Introduction

Recently developed mass spectrometric [1, 2] and optical techniques [3, 4] allow the determination of intramolecular (position-dependent) nitrogen isotope ratios in nitrous oxide (N_2O). The additional information obtained from the intramolecular ratios is complementary to conventional measurements of $^{18}O/^{16}O$ and average $^{15}N/^{14}N$ isotope ratios and may provide deeper insight into stratospheric chemical processes [5, 6, 7, 8, 9, 10] and microbial N_2O sources [11, 12, 13, 14, 15].

Mass spectrometric analysis of position-dependent $^{15}N/^{14}N$ isotope ratios relies on measurements of NO^+ fragment ions that are produced from N_2O in the electron impact ion source. Therefore, ion current ratios at mass-to-charge ratios (m/z) 30 and 31 are monitored. Ideally, m/z 31 fragments should originate from $^{14}N^{14}N^{17}O$ and $^{14}N^{15}N^{16}O$. However, isotopic scrambling in the ion source produces not only $^{15}N^{16}O^+$ ions from $^{14}N^{15}N^{16}O$, but also $^{14}N^{16}O^+$ ions (and vice versa for $^{15}N^{14}N^{16}O$), presumably via a cyclic inter-

mediate. Such an effect was noted by Friedman and Bigeleisen [16] and has to be accounted for in the calculation of the position-dependent isotope ratios of N_2O. In contrast, optical methods measure the relative abundance of isotopically substituted N_2O molecules directly via their characteristic infrared absorption lines, but do not achieve the same precision as mass spectrometry.

Both mass spectrometric and optical methods are based on isotope ratio measurements relative to a reference gas. Unfortunately, no internationally recognized N_2O reference material of known absolute isotopic composition exists. Therefore, the reference gases of individual laboratories have to be traced back by adequate chemical conversions to the primary isotopic reference materials atmospheric nitrogen (abbreviated air–N_2) for nitrogen isotope ratios and Vienna Standard Mean Ocean Water (VSMOW) for oxygen isotope ratios (e.g., [17]). The isotope ratios of these primary isotopic reference materials have been measured on carefully calibrated mass spectrometers [18, 19, 20, 21, 22].

Additional efforts are required, however, to retrieve the position-dependent nitrogen isotope information, because it is lost by conversion of N_2O to N_2. Thermodynamic equilibration of the N_2O isotopomers in the reference gas is not a viable approach, because the equilibrium isotope fractionation between the two non-equivalent nitrogen atoms remains large up to the decomposition temperature of N_2O [23]. Therefore, Toyoda and Yoshida [1] considered four procedures for a position-dependent calibration of N_2O reference gases:

1. Synthesis of N_2O from NH_4NO_3 with known nitrogen isotope ratios in ammonium and nitrate
2. Measurement relative to pure NO of known isotopic composition
3. Preparation of calibrated N_2O mixtures from $^{14}N^{15}NO$, $^{15}N^{14}NO$, and $^{14}N_2O$
4. Infrared absorption spectroscopy

Toyoda and Yoshida [1] actually used the first two methods for calibration of their reference gas. The first approach requires laborious wet chemistry and attention to potential isotope fractionation effects due to incomplete conversion and by-product formation. The second approach is motivated by the use of the NO^+ fragment ion for mass spectrometric position-dependent ^{15}N measurements, but was impaired by the different ionization conditions for NO and N_2O gas in the ion source. The third approach was rejected because commercially available samples of high isotopic purity were lacking. The fourth approach would require absolute isotope ratio measurements by optical spectroscopy at natural abundance levels of ^{15}N, which is currently not possible with the desired precision of less than 1‰.

Sutka et al. [24] used the third approach to calibrate their reference gas. Different amounts of $N^{15}NO$ were added to the reference gas, and the isotope ratio at the central nitrogen position of the mixture was plotted against the molar fraction of $N^{15}NO$ in the N_2O mixture. The ordinate intercept corresponds to the isotope ratio at the central nitrogen position of the reference gas. However, we note that the authors neither measured the isotopic purity of their $^{14}N^{15}NO$ gas nor did they use the accurate mixing relationship for isotope ratios [25]. Moreover, their data show rather large scatter that might be attributed to the volumetric preparation of the gas mixture, and the slope of the linear regression line is about a factor of two smaller than the expected slope (see "Appendix A").

Here we describe yet another method to obtain absolute position-dependent information on an N_2O reference gas by a purely mass spectrometric technique. By using a dual-inlet system, this method can be implemented in less than a day and has a precision comparable to the calibration by NH_4NO_3 decomposition. The method consists of addition of pure $^{15}N_2O$ to the N_2O reference gas and mass spectrometric measurement of $^{45}\delta$, $^{46}\delta$, and $^{31}\delta$, that is, the isotope ratios of N_2O^+ and NO^+ ions (m/z 44, 45, 46 and m/z 30, 31) in the mixture relative to those in the reference gas. $^{45}\delta$ is monitored as a control for a possible contamination of $^{15}N_2O$ by $^{14}N^{15}N^{16}O$ and $^{15}N^{14}N^{16}O$. This procedure avoids gravimetric, manometric, or volumetric preparation of calibrated gas mixtures, which are difficult to accomplish by conventional techniques with the required precision of less than 1‰. Rather, the isotope ratio mass spectrometer itself is used as a tool for calibration that can measure relative isotope ratios with a precision of approximately 10^{-5}.

Theory

The calibration procedure is based on a series of mixtures of the reference gas with doubly labeled N_2O (i.e., $^{15}N_2O$). Isotopic purity was ascertained by mass spectrometry and infrared absorption spectroscopy (see below). More than 99.5% of the doubly labeled N_2O of the Mainz/Heidelberg group (authors Kaiser, Brenninkmeijer, Röckmann) is indeed $^{15}N_2{}^{16}O$, but small contributions of $^{15}N^{14}N^{16}O$ and $^{14}N^{15}N^{16}O$ are also present, which were corrected for in the final calibration. The $^{15}N_2{}^{16}O$ abundance in the doubly labeled N_2O sample of the Berkeley group (authors Park, Boering) was about 98%, so that larger corrections are required (see "Appendix D: purity of the $^{15}N_2O$ samples"). Whenever we want to make a distinction between the Mainz/Heidelberg and Berkeley groups involved in this paper, we will indicate this by "MPI" and "UCB", respectively. Measurements performed at Thermo Finnigan MAT, Bremen, will be referred to as "Bremen". For convenience, we first develop the theoretical background of the calibration technique assuming a pure $^{15}N_2O$ sample. Oxygen isotopes in $^{15}N_2O$ were at their natural abundance (0.04% ^{17}O and 0.21% ^{18}O). We investigate the influence of impurities later.

The addition of $^{15}N_2{}^{16}O$ to a N_2O gas sample influences the ion currents at both m/z 46 and m/z 31. Their co-variation can be exploited by measuring $^{31}R_{\mathrm{ref}}$ if $^{46}R_{\mathrm{ref}}$ is known. $^{46}R_{\mathrm{ref}}$ is the "molecular isotope ratio" of mass-46 to mass-44 species in the reference gas, that is, $[x(^{14}N_2{}^{18}O)+x(^{14}N^{15}N^{17}O)+x(^{15}N^{14}N^{17}O)+x(^{15}N_2{}^{16}O)]/x(^{14}N_2{}^{16}O)$, with x values representing amount fractions. $^{31}R_{\mathrm{ref}}$ is defined anal-

ogously as [x(N^{15}N^{16}O)+x(N^{14}N^{17}O)]/x(N^{14}N^{16}O) where isotopically unspecified atoms are understood to comprise all isotopes (e.g., N^{15}N^{16}O consists of ^{14}N^{15}N^{16}O and ^{15}N$_2$^{16}O). The idea behind using ^{15}N$_2$O is that isotopic scrambling during NO$^+$ formation in the ion source does not play a role, because species of mass 31 will be formed in any case.

The isotope ratios of the reference gas are given by the following equations [17].

$$^{45}R_{\mathrm{ref}} = {}^{15}R_{1,\mathrm{ref}} + {}^{15}R_{2,\mathrm{ref}}\,{}^{17}R_{\mathrm{ref}} \tag{1}$$

$$^{46}R_{\mathrm{ref}} = \left({}^{15}R_{1,\mathrm{ref}} + {}^{15}R_{2,\mathrm{ref}}\right){}^{17}R_{\mathrm{ref}} + {}^{18}R_{\mathrm{ref}} + {}^{15}R_{1,\mathrm{ref}}\,{}^{15}R_{2,\mathrm{ref}} \tag{2}$$

$$^{31}R_{\mathrm{s,ref}} = \frac{s\,{}^{15}R_{1,\mathrm{ref}} + (1-s)\,{}^{15}R_{2,\mathrm{ref}} + {}^{15}R_{1,\mathrm{ref}}\,{}^{15}R_{2,\mathrm{ref}}}{1 + s\,{}^{15}R_{2,\mathrm{ref}} + (1-s)\,{}^{15}R_{1,\mathrm{ref}}} + {}^{17}R_{\mathrm{ref}} \tag{3}$$

The symbol s denotes the "scrambling coefficient", that is, the proportion of NO$^+$ fragment ions with an N atom originating from the terminal N atom in N$_2$O. $^{15}R_{1,\mathrm{ref}}$ and $^{15}R_{2,\mathrm{ref}}$ are the elemental isotope ratios of the terminal and central nitrogen atom, respectively. $^{17}R_{\mathrm{ref}}$ and $^{18}R_{\mathrm{ref}}$ are the oxygen isotope ratios. The index "s" in Eq. 3 stands for "scrambled". The term $^{15}R_{1,\mathrm{ref}}{}^{15}R_{2,\mathrm{ref}}$ in Eqs. 2 and 33 represents the statistically expected contribution of ^{15}N$_2$^{16}O in the reference gas. The term $1+s^{15}R_{2,\mathrm{ref}}+(1-s)^{15}R_{1,\mathrm{ref}}$ in Eq. 3 arises from the production of ^{14}N^{16}O$^+$ by ^{14}N$_2$^{16}O, ^{14}N^{15}N^{16}O, and ^{15}N^{14}N^{16}O, because scrambling not only effects ion currents at m/z 31, but also at m/z 30. If ^{15}N$_2$^{16}O is added to the reference gas, the abundance of ^{15}N$_2$^{16}O is higher than the statistically expected contribution. The excess ^{15}N$_2$^{16}O is expressed by the symbol $^{15}R_{1+2}$. $^{15}R_{1+2}$ equals the ratio of ^{15}N$_2$^{16}O (from doubly labeled N$_2$O) to ^{14}N$_2$^{16}O (from the reference gas) in the mixture. The isotope ratios of the labeled mixture are therefore

$$^{45}R = {}^{15}R_{1,\mathrm{ref}} + {}^{15}R_{2,\mathrm{ref}} + {}^{17}R_{\mathrm{ref}} = {}^{45}R_{\mathrm{ref}} \tag{4}$$

$$\begin{aligned} ^{46}R &= \left({}^{15}R_{1,\mathrm{ref}} + {}^{15}R_{2,\mathrm{ref}}\right){}^{17}R_{\mathrm{ref}} + {}^{18}R_{\mathrm{ref}} + {}^{15}R_{1,\mathrm{ref}}\,{}^{15}R_{2,\mathrm{ref}} \\ &\quad + {}^{15}R_{1+2} = {}^{46}R_{\mathrm{ref}} + {}^{15}R_{1+2} \end{aligned} \tag{5}$$

$$\begin{aligned} ^{31}R_{\mathrm{s}} &= \frac{s\,{}^{15}R_{1,\mathrm{ref}} + (1-s)\,{}^{15}R_{2,\mathrm{ref}} + {}^{15}R_{1,\mathrm{ref}}\,{}^{15}R_{2,\mathrm{ref}} + {}^{15}R_{1+2}}{1 + s\,{}^{15}R_{2,\mathrm{ref}} + (1-s)\,{}^{15}R_{1,\mathrm{ref}}} \\ &\quad + {}^{17}R_{\mathrm{ref}} = {}^{31}R_{\mathrm{s,ref}} + \frac{{}^{15}R_{1+2}}{1 + s\,{}^{15}R_{2,\mathrm{ref}} + (1-s)\,{}^{15}R_{1,\mathrm{ref}}} \end{aligned} \tag{6}$$

^{45}R is identical to $^{45}R_{\mathrm{ref}}$ if the ^{15}N$_2$O sample does not contain any other isotopologues. The expected relationship between $^{46}\delta$ and $^{31}\delta$ can then be calculated from Eqs. 2, 3, 5, and 6:

$$^{46}\delta = \frac{^{46}R}{^{46}R_{\mathrm{ref}}} - 1 = \frac{^{15}R_{1+2}}{^{46}R_{\mathrm{ref}}} \tag{7}$$

$$\begin{aligned} ^{31}\delta &= \frac{^{31}R_{\mathrm{s}}}{^{31}R_{\mathrm{s,ref}}} - 1 = \frac{^{15}R_{1+2}}{^{31}R_{\mathrm{s,ref}}\left[1 + s\,{}^{15}R_{2,\mathrm{ref}} + (1-s)\,{}^{15}R_{1,\mathrm{ref}}\right]} \\ &= \frac{^{46}R_{\mathrm{ref}}\,{}^{46}\delta}{^{31}R_{\mathrm{s,ref}}\left[1 + s\,{}^{15}R_{2,\mathrm{ref}} + (1-s)\,{}^{15}R_{1,\mathrm{ref}}\right]} \end{aligned} \tag{8}$$

A plot of $^{31}\delta$ versus $^{46}\delta$ gives $\frac{^{46}R_{\mathrm{ref}}}{^{31}R_{\mathrm{s,ref}}\left[1 + s\,{}^{15}R_{2,\mathrm{ref}} + (1-s)\,{}^{15}R_{1,\mathrm{ref}}\right]}$ as the slope, which can be used in conjunction with Eq. 3 to derive $^{15}R_{1,\mathrm{ref}}$ and $^{15}R_{2,\mathrm{ref}}$ if s, $^{46}R_{\mathrm{ref}}$, $^{17}R_{\mathrm{ref}}$, and $^{15}R_{\mathrm{ref}}$ are known. $^{15}R_{\mathrm{ref}}$ is the average ^{15}N/^{14}N isotope ratio defined as ($^{15}R_{1,\mathrm{ref}}$+$^{15}R_{2,\mathrm{ref}}$)/2. $^{17}R_{\mathrm{ref}}$ can be calculated from $^{18}R_{\mathrm{ref}}$ if a mass-dependent relationship of the form $^{17}R_{\mathrm{ref}}=A(^{18}R_{\mathrm{ref}})^{\beta}$ is assumed. Both $^{15}R_{\mathrm{ref}}$ and $^{18}R_{\mathrm{ref}}$ are accessible by "conventional" calibration of the N$_2$O reference gas.

Next, we consider the influence of impurities in the doubly labeled N$_2$O sample. As determined in "Appendix D: purity of the ^{15}N$_2$O samples", the only relevant impurities for our experiments are CO$_2$ (at m/z 44, 45, 46) and ^{15}N^{14}N^{16}O and ^{14}N^{15}N^{16}O (at m/z 30, 31, and 45). Other sources of CO$_2$ can be leaks of the sample containers or a CO$_s$ background in the mass spectrometer. Furthermore, ^{15}N$_2^+$ formation from ^{15}N$_2$O has to be taken into account for the m/z 30 ion current.

Interferences from CO$_2$ can be accounted for by the measurement of interfering masses at m/z 12 (corresponding to ^{12}C$^+$) as explained in detail by Kaiser et al. [17]. Based on their Eqs. 17a and 17b, the raw $^{45}\delta'$ and $^{46}\delta'$ values can be corrected as follows:

$$^{45}\delta = \left(1 + {}^{45}\delta'\right)\frac{1 - \frac{^{45}u}{^{45}U'}}{1 - \frac{^{44}u}{^{44}U'}}\frac{1 - \frac{^{44}v}{^{44}V'}}{1 - \frac{^{45}v}{^{45}V'}} - 1 \tag{9a}$$

$$^{46}\delta = \left(1 + {}^{46}\delta'\right)\frac{1 - \frac{^{46}u}{^{46}U'}}{1 - \frac{^{44}u}{^{44}U'}}\frac{1 - \frac{^{44}v}{^{44}V'}}{1 - \frac{^{46}v}{^{46}V'}} - 1 \tag{9b}$$

U' and V' are the actually measured voltages at m/z 44, 45, and 46 (produced by the ion currents on the amplifier feedback resistors) for sample and reference, respectively. They are the sum of the true voltages U and V for N$_2$O only and the voltages due to CO$_2$ interference, u and v (e.g., $^{45}U'=^{45}U+^{45}u$). Assuming that the contaminating CO$_2$ is always of the same isotopic composition, ^{45}u and ^{46}u are related to ^{44}u via $^{45}u=^{44}u\,^{45}R(\mathrm{CO_2})\,^{45}k$ and $^{46}u=^{44}u\,^{46}R(\mathrm{CO_2})\,^{46}k$ (analogously for ^{45}v and ^{46}v). $^{45}R(\mathrm{CO_2})$ and $^{46}R(\mathrm{CO_2})$ are the "molecular" isotope ratios of CO$_2$. ^{45}k and ^{46}k measure the overall mass discrimination in 45/44 and 46/44 analysis, respectively. In the case of N$_2$O, ^{45}k and ^{46}k are equal to $1/^{45}R_{\mathrm{ref}}\,{}^{45}U/{}^{44}U$ and $1/^{46}R_{\mathrm{ref}}\,{}^{46}U/{}^{44}U$. Assuming that the overall mass discrimination is the same for CO$_2$ and N$_2$O, Eqs. 9a and 9b can be rearranged to:

$$^{45}\delta = \frac{\left(1 + {}^{45}\delta'\right)\left(1 - \frac{^{45}u}{^{45}U'}\right)}{1 + \frac{^{45}v}{^{45}V'}\left(\frac{^{45}R_{\mathrm{ref}}}{^{45}R(\mathrm{CO_2})} - 1\right) - \frac{^{45}u}{^{45}V'}\frac{^{44}V'}{^{44}U'}\frac{^{45}R_{\mathrm{ref}}}{^{45}R(\mathrm{CO_2})}} - 1 \tag{10a}$$

$$^{46}\delta = \frac{\left(1 + {}^{46}\delta'\right)\left(1 - \frac{^{46}u}{^{46}U'}\right)}{1 + \frac{^{46}v}{^{46}V'}\left(\frac{^{46}R_{\mathrm{ref}}}{^{46}R(\mathrm{CO_2})} - 1\right) - \frac{^{46}u}{^{46}V'}\frac{^{44}V'}{^{44}U'}\frac{^{46}R_{\mathrm{ref}}}{^{46}R(\mathrm{CO_2})}} - 1 \tag{10b}$$

^{44}u and ^{44}v can be inferred from the voltage of interfering mass 12 measured on the m/z 46 cup (^{12}u and ^{12}v, respectively) if the relative intensity of the $^{12}C^+$ and $^{12}C^{16}O$ ion currents in the CO_2 mass spectrum are known. By Defining ^{12}r as $^{12}u/(^{44}u^{46}k)$, we find that ^{12}r equals 3.9±0.1% on our instrument. We assume that the isotopic composition of the contaminating CO_2 corresponds to tropospheric CO_2 with $\delta^{13}C$=–8‰ and $\delta^{18}O$=0‰ versus VPDB–CO_2 [26, 27]. $^{45}R(CO_2)$ is therefore 0.01191 and $^{46}R(CO_2)$ is 0.00419. Then Eqs. 10a and 10b can be used to calculate the unbiased $^{45}\delta$ and $^{46}\delta$ values. The approximate versions of these equations described by Kaiser et al. [17] cannot be applied in the present case because of the large enrichments of the sample relative to the reference.

Interferences by $^{15}N^{14}N^{16}O$ and $^{14}N^{15}N^{16}O$ and $^{15}N_2^+$ formation from ^{15}NO are incorporated explicitly into modified versions of Eqs. 3, 4, and 6. ^{46}R remains unchanged from Eq. 5.

$$^{45}R = {}^{45}R_{\mathrm{ref}} + {}^{15}R_{\mathrm{l+2}}\left({}^{15}Z_1 + {}^{15}Z_2\right) \tag{11}$$

$$^{31}R_{\mathrm{s,ref}} = \frac{\begin{array}{c} s\,{}^{15}R_{\mathrm{l,ref}} + (1-s)\,{}^{15}R_{\mathrm{2,ref}} + {}^{15}R_{\mathrm{l,ref}}\,{}^{15}R_{\mathrm{2,ref}} \\ + {}^{17}R_{\mathrm{ref}}\left[1 + s\,{}^{15}R_{\mathrm{2,ref}} + (1-s)\,{}^{15}R_{\mathrm{l,ref}}\right] \end{array}}{1 + s\,{}^{15}R_{\mathrm{2,ref}} + (1-s)\,{}^{15}R_{\mathrm{l,ref}} + p\,{}^{15}R_{\mathrm{l,ref}}\,{}^{15}R_{\mathrm{2,ref}}} \tag{12}$$

$$^{31}R_{\mathrm{s}} = \frac{\begin{array}{c} s\,{}^{15}R_{\mathrm{l,ref}} + (1-s)\,{}^{15}R_{\mathrm{2,ref}} + {}^{15}R_{\mathrm{l,ref}}\,{}^{15}R_{\mathrm{2,ref}} \\ + {}^{17}R_{\mathrm{ref}}\left[1 + s\,{}^{15}R_{\mathrm{2,ref}} + (1-s)\,{}^{15}R_{\mathrm{l,ref}}\right] \\ + \left[1 + (1-s)Z_2 + sZ_1\right]{}^{15}R_{\mathrm{l+2}} \end{array}}{\begin{array}{c} 1 + s\,{}^{15}R_{\mathrm{2,ref}} + (1-s)\,{}^{15}R_{\mathrm{l,ref}} + p\,{}^{15}R_{\mathrm{l,ref}}\,{}^{15}R_{\mathrm{2,ref}} \\ + \left[(1-s)Z_1 + sZ_2 + p\right]{}^{15}R_{\mathrm{l+2}} \end{array}} \tag{13}$$

$^{15}R_{1+2}$ equals $N_C(^{15}N_2{}^{16}O)/N_{\mathrm{ref}}(^{14}N_2{}^{16}O)$, $^{15}Z_1$ is $N_C(^{15}N^{14}N^{16}O)/N_C(^{15}N_2{}^{16}O)$, and $^{15}Z_2$ is $N_C(^{14}N^{15}N^{16}O)/N_C(^{15}N_2{}^{16}O)$, where N_C and N_{ref} are the number of molecules from doubly labeled N_2O and the reference gas, respectively. The coefficient p represents the abundance of $^{15}N_2^+$ ions relative to the abundance of $^{15}N_2{}^{16}O^+$. The value of p varied slightly for different mass spectrometers and was 10.5% (MPI), 10% (Bremen), and 15% (UCB). For the δ values, we get

$$^{45}\delta = {}^{15}R_{\mathrm{l+2}}\,\frac{{}^{15}Z_1 + {}^{15}Z_2}{{}^{45}R_{\mathrm{ref}}} \tag{14}$$

$$^{31}\delta = \frac{{}^{15}R_{\mathrm{l+2}}}{{}^{31}R_{\mathrm{s,ref}}}\,\frac{\begin{array}{c} 1 + s\,{}^{15}Z_1 + (1-s)\,{}^{15}Z_2 \\ - {}^{31}R_{\mathrm{s,ref}}\left[(1-s)\,{}^{15}Z_1 + s\,{}^{15}Z_2 + p\right] \end{array}}{\begin{array}{c} 1 + s\,{}^{15}R_{\mathrm{2,ref}} + (1-s)\,{}^{15}R_{\mathrm{l,ref}} + p\,{}^{15}R_{\mathrm{l,ref}}\,{}^{15}R_{\mathrm{2,ref}} \\ + {}^{15}R_{\mathrm{l+2}}\left[(1-s)\,{}^{15}Z_1 + s\,{}^{15}Z_2 + p\right] \end{array}} \tag{15}$$

$$^{31}\delta \approx \frac{{}^{15}R_{\mathrm{l+2}}}{{}^{31}R_{\mathrm{s,ref}}}\,\frac{1 + s\,{}^{15}Z_1 + (1-s)\,{}^{15}Z_2 - {}^{31}R_{\mathrm{s,ref}}\,p}{1 + s\,{}^{15}R_{\mathrm{2,ref}} + (1-s)\,{}^{15}R_{\mathrm{l,ref}} + p\,{}^{15}R_{\mathrm{l+2}}} \tag{16}$$

The approximation only neglects quantities which are of the order of 10^{-5} times the δ value or smaller: the product of $^{15}R_{1+2}$ and $^{15}Z_1$ or $^{15}Z_2$ never exceeded 2×10^{-5}. Such corrections are significantly below the measurement precision and can therefore be neglected. Equation 7 can be substituted into Eq. 14 and the relationship between $^{45}\delta$ and $^{46}\delta$ is then used to estimate $^{15}Z_1$+$^{15}Z_2$:

$$^{45}\delta = {}^{46}R_{\mathrm{ref}}\,\frac{{}^{15}Z_1 + {}^{15}Z_2}{{}^{45}R_{\mathrm{ref}}}\,{}^{46}\delta \tag{17}$$

An assumption has to be made concerning the ratio of $^{15}Z_1/^{15}Z_2$, but the final result for $^{15}R_{1,\mathrm{ref}}$ and $^{15}R_{2,\mathrm{ref}}$ is not very sensitive to this assumption. In the most likely case, ^{15}N is assumed to be distributed symmetrically over $^{15}N^{14}N^{16}O$ and $^{14}N^{15}N^{16}O$, as discussed below, so that $^{15}Z_1/^{15}Z_2$ is close to 1. By substituting $^{15}Z_1$=$^{15}Z_2$ and Eq. 7 into Eq. 16, we then have for $^{31}\delta$

$$^{31}\delta \approx \frac{{}^{46}R_{\mathrm{st}}}{{}^{31}R_{\mathrm{s,ref}}}\,\frac{1 + {}^{15}Z_1 - {}^{31}R_{\mathrm{s,ref}}\,p}{1 + s\,{}^{15}R_{\mathrm{2,ref}} + (1-s)\,{}^{15}R_{\mathrm{l,ref}} + {}^{46}R_{\mathrm{ref}}\,p\,{}^{46}\delta}\,{}^{46}\delta \tag{18}$$

Due to $^{15}N_2{}^+$ production, the term $^{46}R_{\mathrm{ref}}p^{46}\delta$ appears in the denominator of Eq. 18, and $^{31}\delta$ is no longer directly proportional to $^{46}\delta$. Therefore, the slope of a plot of $^{31}\delta$ versus $^{46}\delta$ is not constant, but decreases with increasing $^{46}\delta$. Equation 18 can be expanded in terms of $^{46}\delta$. There is no ordinate intercept, and for the coefficient of the linear term we obtain $\dfrac{{}^{46}R_{\mathrm{ref}}\left(1 + {}^{15}Z_1 - {}^{31}R_{\mathrm{s,ref}}\,p\right)}{{}^{31}R_{\mathrm{s,ref}}\left[1 + s\,{}^{15}R_{\mathrm{2,ref}} + (1-s)\,{}^{15}R_{\mathrm{l,ref}}\right]}$.

Obviously, the result of the calibration depends not only on the slope of the $^{31}\delta$ versus $^{46}\delta$ plot, but also on the conventional absolute isotope ratios of the reference ($^{15}R_{\mathrm{ref}}$, $^{17}R_{\mathrm{ref}}$, $^{18}R_{\mathrm{ref}}$) and, therefore, ultimately on the accuracy of the isotope ratios of the primary isotopic reference materials.

Table 1 shows the absolute isotope ratios used in the calculations here. For ^{17}R(VSMOW) we use primarily the value of Li et al. [20], but also demonstrate the impact of a more recent calibration of ^{17}R(VSMOW) by Assonov and Brenninkmeijer [21] and the value for ^{17}R(VSMOW)

Table 1 Overview of primary isotopic reference materials and their absolute isotope ratios used in this paper

Species	Scale	$R/10^{-6}$	Relative error (‰)	Reference
$^{13}C/^{12}C$	VPDB[a]	11180±28	2.5	[41]
$^{15}N/^{14}N$	Air–N_2	3678.2±1.5	0.4	[22]
	Air–N_2	3676.5±4.1[c]	1.1	[18]
$^{17}O/^{16}O$	VSMOW	379.9±0.8	2.1	[20]
	VSMOW	384.7±0.9[b]	2.2	[21]
	VSMOW	372±4	11	[20, 28, 29]
$^{18}O/^{16}O$	VSMOW	2005.2±0.45	0.2	[19]

[a] *VPDB* Vienna Pee Dee Belemnite
[b] This value has been re-scaled from the value of ^{13}R(VPDB)= 0.0112372 [28] used by Assonov and Brenninkmeijer [21] to a more recent absolute calibration of ^{13}R(VPDB) [41]
[c] This is the value recommended by IUPAC for reporting of the nitrogen isotope abundance [42]. However, for our calculations we prefer the more precise determination by De Bièvre et al. [22], which agrees with the recommended value within the error

Table 2 Overview of the N_2O samples used for different mixing series

	MPI-1[a] (reference gas) (‰)	MPI-2[a] (‰)	UCB-N_2O (reference gas) (‰)
δ^{15}N verus air–N_2	1.01±0.03[b]	–1.77±0.03	0.15±0.04
δ^{18}O versus VSMOW	38.45±0.22[b]	40.47±0.22	41.69±0.22
$^{45}\delta$ versus MPI-1	0	–2.59±0.01	–0.73±0.02
$^{46}\delta$ versus MPI-1	0	1.89±0.02	3.08±0.03
$^{31}\delta$ versus MPI-1	0	8.51±0.08	–0.72±0.54

[a]MPI-1 is ultra-high purity N_2O (Messer Griesheim, grade 6.0). MPI-2 is an N_2O sample derived from adipic acid production (Puritan-Bennet Medical Gases, grade 2.2). UCB-N_2O is of grade 4.7 purity (Scott Specialty Gases)
[b]See Kaiser et al. [17] for details of the absolute calibration

derived from Craig's classic paper [28], using the relationships recommended by the IAEA for the oxygen isotope ratios of VPDB–CO_2 and VSMOW [29]. The ^{17}R, ^{18}R, and average ^{15}R isotope ratios of the MPI-1 reference gas have been calibrated relative to VSMOW and air–N_2 [17]. In Table 4, we will show in detail which influence the uncertainties of the individual quantities used for the calibration have on the final result for the position-dependent isotope ratios of the N_2O reference gas. The $^{45}\delta$, $^{46}\delta$, and $^{31}\delta$ values of a secondary reference gas (MPI-2) and the UCB reference gas have been measured relative to MPI-1 (Table 2). δ^{18}O as well as the position-dependent δ^{15}N values ($^{1}\delta^{15}$N and $^{2}\delta^{15}$N, for terminal and central nitrogen atom, respectively) were calculated by using the data reduction procedure of Kaiser et al. [17]. ^{17}R is calculated from a mass-dependent relationship with ^{18}O (i.e., $^{17}R=A(^{18}R)^{\beta}$ with β=0.516 and A=0.00937035) [17].

Experimental results

In this section, we will first explain how the scrambling coefficient s was determined. It is crucial to all position-dependent isotope measurements of N_2O, but we will show in the discussion of our results that the observed variations of s have only a small influence on the uncertainty of the final position-dependent nitrogen isotope ratios. Then, the results from an intercomparison of a set of seven enriched samples prepared at UCB are shown, measured on three different mass spectrometers. The MPI and UCB measurements for the present study were performed on nearly identical Finnigan MAT 252 mass spectrometers, the measurements at Thermo Finnigan MAT in Bremen were done with a MAT 253 instrument. All instruments were operated in dual-inlet mode. The MAT 252 instruments did not have a dedicated Faraday cup configuration for analyses at m/z 30 and 31, but accurate $^{31}\delta$ values can be obtained even with the O_2 cup configuration (cups for m/z 32 and 33; Fig. 2). Finally, results for different mixing series of doubly labeled N_2O with the MPI-1, MPI-2, and UCB reference gases prepared at different times and measured with different mass spectrometers will be presented, and the position-dependent nitrogen isotope ratios are calculated. In principle, it would be sufficient to measure the $^{45}\delta$, $^{46}\delta$, and $^{31}\delta$ values of a single $^{15}N_2O$-enriched sample relative to the reference gas to derive the absolute position-dependent ratios, but we prefer to use a mixing series to make our results more robust.

Determination of the scrambling coefficient *s*

The scrambling coefficient s for the MPI analyses was determined on commercial samples of ^{15}NNO and N^{15}NO (ICON Isotopes, Summit, NJ, USA). The purity of these samples was ascertained by mass spectrometry and Fourier transform infrared spectroscopy (FTIR). According to the mass spectrometric analyses the samples contained amount fractions of 0.36–0.39% $^{14}N_2{}^{16}O$, 98.96–98.99% $^{14}N^{15}N^{16}O$+$^{15}N^{14}N^{16}O$, 0.44% $^{15}N_2{}^{16}O$+$^{14}N^{15}N^{17}O$+$^{15}N^{14}N^{17}O$, and 0.21% $^{14}N^{15}N^{18}O$+$^{15}N^{14}N^{18}O$. Contamination of the sample by CO_2 was less than 0.01% and therefore negligible. FTIR proved that the isotopomeric purity (i.e., the contribution of the isotopomer stated on the commercial product compared to the sum of $^{14}N^{15}N^{16}O$+$^{15}N^{14}N^{16}O$) was ≥99.9%. The value of 0.21% for $^{14}N^{15}N^{18}O$+$^{15}N^{14}N^{18}O$ showed that oxygen isotope ratios were normal. Because of the low $^{14}N_2{}^{16}O$ abundance, contributions by $^{14}N_2{}^{17}O$ and$^{14}N_2{}^{18}O$ were negligible. The scrambling coefficient can be determined essentially from the ratio of ion currents at m/z 31 and m/z 30 for $^{15}N^{14}N^{16}O$ and the reciprocal ratio for $^{14}N^{15}N^{16}O$. However, corrections have to be applied for the contribution of $^{14}N_2{}^{16}O$ to m/z 30 as well as for $^{15}N_2{}^{16}O$ and $^{15}N^{14}N^{17}O$ to m/z 31 ($^{15}N^{14}N^{17}O$ is only relevant for $^{15}N^{14}N^{16}O$). Assuming a $^{17}O/^{16}O$ ratio of 0.00039 and the above contributions from undesired N_2O species, the corrections amount to a change in the raw 31/30 ratio from, for example, s=8.60% to s=8.23% for $^{15}N^{14}NO$. Under normal mass spectrometric conditions, we found a value of s=8.22±0.01% that was very stable over time, although we note that s was significantly lower, namely 7.89±0.01%, when an aged filament was used. Allowing for a 0.1% cross-contamination by the other than the desired isotopomer results in a relative decrease of s by about 1%, which is negligible for the precision of the final position-dependent analysis.

For the analyses at UCB, a scrambling coefficient of 8.46% was determined. Toyoda and Yoshida [1] found 8.11±0.01% on their MAT 252 mass spectrometer. Because the ion sources of the MAT 253 and 252 mass spectrometers are similar in design and because s always seems to be about 8% for different mass spectrometers [16, 30], we adopt value of s=8.2% for the MAT 253 mass spectrometer in Bremen. Other ion source parameters (like electron energy or extraction voltage) had a minor influence on s, but in any case, the observed variation of s was not limiting for the final precision of our intramolecular nitrogen isotope ratios. On a Micromass Isoprime mass spectrometer, Sutka et al. [24] found a much larger

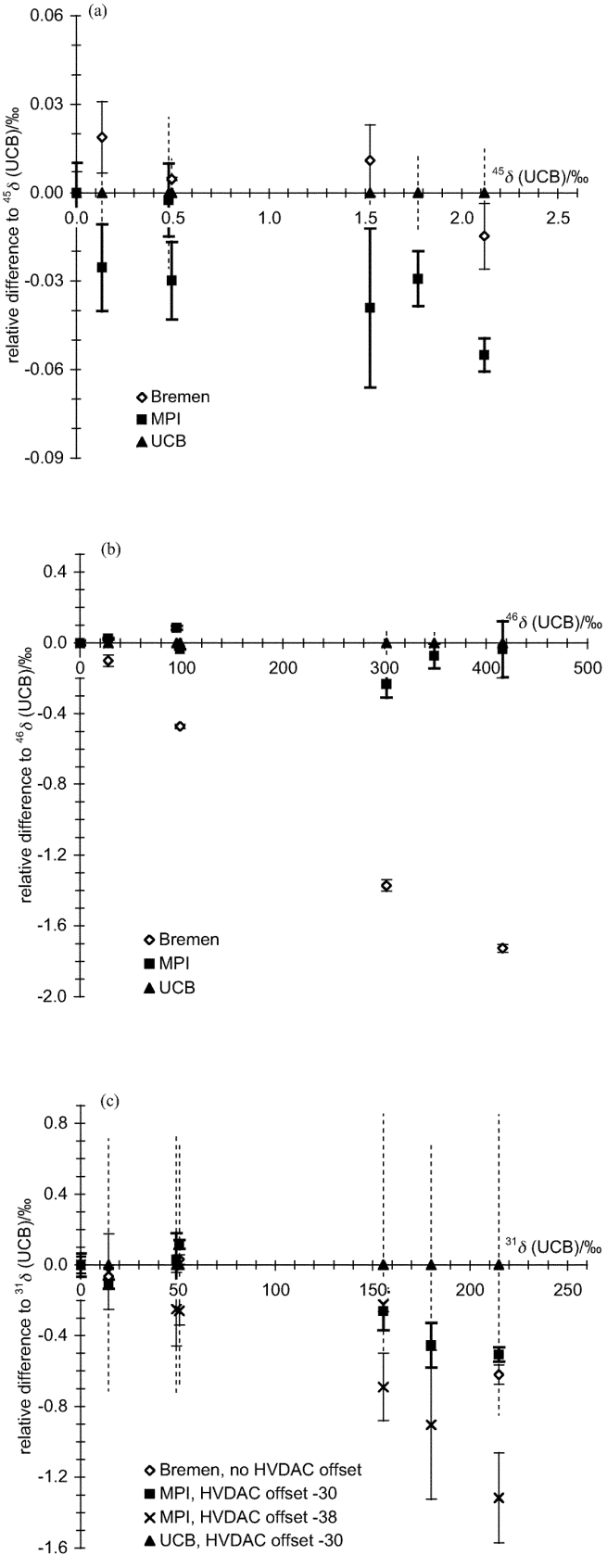

scrambling coefficient of 19.5±1.7%, which they attributed to a higher degree of intramolecular rearrangement in the field-free region between ion source and magnet field. However, if NO^+ production were to occur in this part of the mass spectrometer, one would not observe an NO^+-peak at m/z 30, but the metastable ion peak at m/z 20.45 [31]. In order to explain the difference in s between Sutka et al.'s value of approximately 20% and all other reported values of approximately 8%, quite different conditions in the ion source must be invoked.

Intercomparison of $^{45}\delta$, $^{46}\delta$, and $^{31}\delta$ values

Figure 1 compares measured $^{45}\delta$, $^{46}\delta$, and $^{31}\delta$ values for the same set of seven samples on two MAT 252 (UCB, MPI) and one MAT 253 (Bremen) mass spectrometers. The $^{45}\delta$ values agree very well on all three machines, but the $^{46}\delta$ values measured in Bremen are significantly lower than those measured at UCB and the MPI. This indicates some "scale contraction" for the Bremen machine, possibly due to a small constant NO_2 background or, less likely, due to cross-contamination of sample and reference [32]. To distinguish between the two possibilities, measurements of samples with higher $^{45}\delta$ values should be performed, since the range of $^{45}\delta$ values available here is too small to estimate any cross-contamination effect reliably. We note that a new filament type was used in Bremen that gives higher ion yields per molecule than conventional tungsten filaments and might also produce some NO_2.

The possibility of cross-contamination was studied in detail on the MPI mass spectrometer. Two tests were performed: the normal idle time of 10 s between sequential sample and reference measurements was increased to 120 s, and a series of enriched samples with $^{46}\delta$ values between 0 and 3,000‰ was measured in different combinations of sample and reference gases. Neither test revealed any significant differences for the $^{46}\delta$ value of the most highly enriched sample. We conclude that the MPI and UCB $^{46}\delta$ measurements are most likely accurate and need not be corrected for cross-contamination, whereas the Bremen measurements give values which are systematically too low.

The $^{31}\delta$ values shown in Fig. 1c agree well for the Bremen and MPI measurements when the latter are made with a high-voltage offset of –30 HVDAC units (Fig. 2). Both show small standard deviations of about 0.1‰ or less. The UCB data indicate slightly higher enrichments, but also have larger uncertainties (about 0.7‰). Within

Fig. 1a–c Intercomparison of $^m\delta$ measurements (m=45, 46, 31). $[\delta–\delta(\mathrm{UCB})]/[1+\delta(\mathrm{UCB})]$ is plotted versus δ(UCB) for a set of seven samples. *Error bars* represent the standard deviation of individual δ values. Two sets of $^{31}\delta$ measurements at the MPI are shown, one measured with a high voltage offset of –38 HVDAC units, the other with an offset of –30 HVDAC units (cf. Fig. 2). The UCB measurements shown were also performed with an offset of about –30 HVDAC units

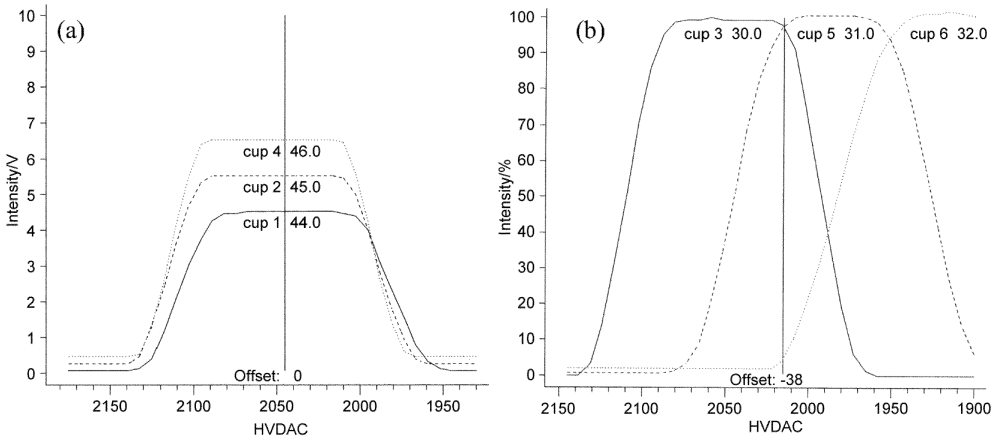

Fig. 2a, b Peak shapes for CO_2 (**a**) and for NO^+ fragment analysis (**b**) on the MPI MAT 252 instrument. N_2O looks similar to CO_2, but with inverse order of voltages. For NO^+ the center of the ion beam does not coincide with the center of the Faraday cup, because the collectors used for NO^+ analysis are intended for analysis of O_2 (*m/z* 32 and 33) rather than NO (*m/z* 30 and 31). In practice, the ion beam is first centered on the mass 30 beam, and then offset to the point of intersection of *m/z* 30 and 31 peaks

the error, they agree with the Bremen and the MPI (offset –30) measurements. In contrast, the MPI values measured with an offset of –38 are significantly lower than the results from the other mass spectrometer configurations. The offset of –38 was chosen for the MPI $^{31}\delta$ measurements, because at this position of the beam, the product of the relative intensities at *m/z* 30 and 31 was maximized [33] (Fig. 2). However, from re-checks of the peak shape after the measurement of some samples, it became apparent that the position of the ion beam sometimes shifts slightly, so that an offset of –30 HVDAC units would be more appropriate, similar to what was used at UCB. As long as an offset of –30 HVDAC units is used, we thus have good agreement for the 252 and 253 measurements. The data from the 253 should represent accurate results, since a proper cup configuration for *m/z* 30, 31 (and 32) was available.

Calibration of the absolute position-dependent nitrogen isotope ratios

Mixing series MPI-1a, MPI-2a, and UCB-a were prepared in June 2002 from mixing of small amounts of MPI-$^{15}N_2O$

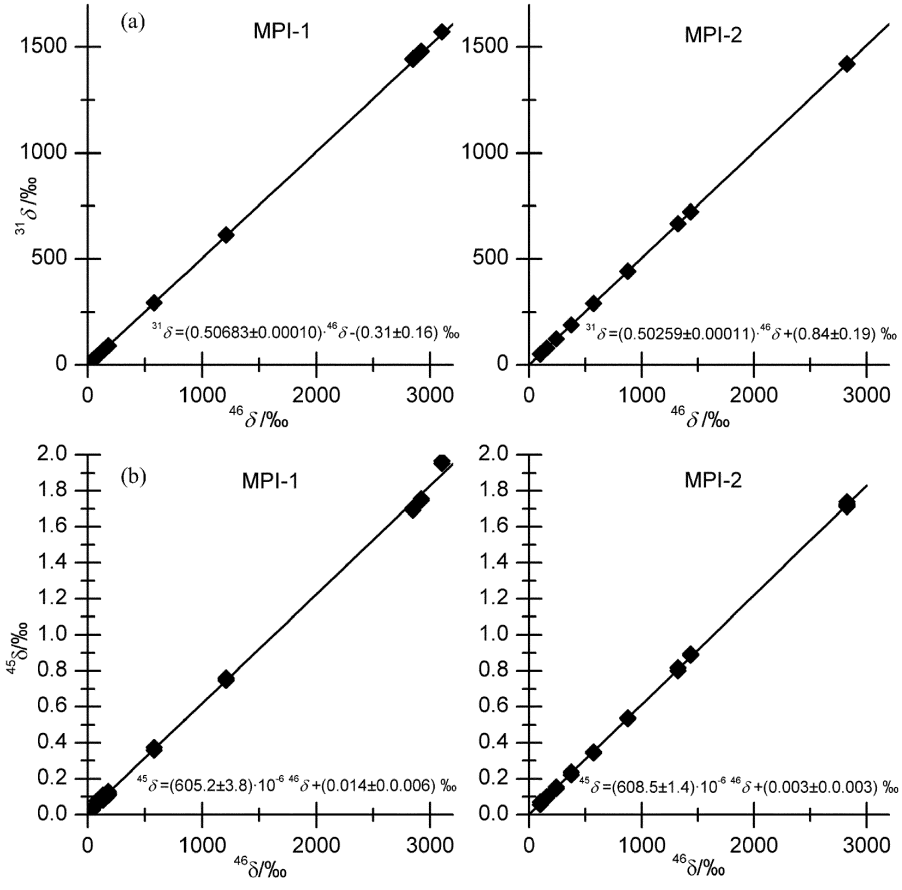

Fig. 3a, b Change of **a** $^{31}\delta$ and **b** $^{45}\delta$ versus $^{46}\delta$ for addition of $^{15}N_2O$ to samples of MPI-1 and MPI-2. Mass spectrometric errors are smaller than the symbol sizes. The slope of these plots can be used derived to the position-dependent ^{15}N isotope ratios of the initial N_2O as described in the main text. Note the change of ordinate scale in **b** compared to **a**

with samples of MPI-1 and MPI-2 as well as from mixing of UCB-$^{15}N_2O$ with the UCB reference gas. Two additional mixing series (MPI-1b and UCB-b) were prepared in May 2003 in the same way.

Figure 3 shows typical plots of $^{31}\delta$ versus $^{46}\delta$ and $^{45}\delta$ versus $^{46}\delta$ for mixtures of MPI-1 and MPI-2 with the MPI-$^{15}N_2O$ sample. Linear least squares regression analyses of $^{31}\delta$ versus $^{46}\delta$ give slopes of 0.50683±0.00010 and 0.50259±0.00011 for MPI-1 and MPI-2; ordinate intercepts are –0.31±0.16‰ and 0.84±0.19‰, respectively. We checked whether it was necessary to consider the mass spectrometric errors in the calculation of the slope, but did not find significant differences to a simple linear least squares regression and therefore chose to use the latter method. We also considered using a quadratic fit rather than a linear one, along the lines of argument following Eq 18. However, the coefficients for the quadratic term showed larger variations, and were sometimes negative and sometimes positive (a negative coefficient would be expected) with standard deviations larger than their actual magnitude. The goodness of fit was not considerably improved over the linear fit either, so that the adequacy of a quadratic fit does not seem to be warranted by the data. A complete overview of the different measurement series is shown in Table 3. Rows 1 and 8 correspond to the data shown in Fig. 3. For simplicity, only the results for MPI-1 are shown, but the values obtained for the MPI-2 and UCB-N_2O reference gases are linked to MPI-1 through direct comparison (Table 2).

Using the $^{31}\delta$ versus $^{46}\delta$ and $^{45}\delta$ versus $^{46}\delta$ slopes, we then proceed to calculate the position-dependent isotope ratios of MPI-1, MPI-2, and UCB-N_2O. Model calculations are performed with the full equations developed earlier (i.e., Eqs. 17 and 18). First, $^{15}Z_1+^{15}Z_2$ is adjusted iteratively to give the $^{45}\delta$ versus $^{46}\delta$ slope, and then the isotope ratio at the terminal nitrogen atom is changed until it gives a $^{31}\delta$ versus $^{46}\delta$ slope consistent with the measured slope.

The results for the $^{1}\delta^{15}$N and $^{2}\delta^{15}$N of MPI-1 agree very well for the pooled measurements with MPI-1 and UCB-N_2O which were both performed on MAT 252 mass spectrometers with HVDAC offsets of –30 (rows 7 and 14, Table 3). Measurements with an HVDAC offset of –38 (rows 1, 2, 4, 6, 8, and 12) give consistent deviations to more negative $^{1}\delta^{15}$N values (and more positive $^{2}\delta^{15}$N values since the average δ^{15}N is fixed). This difference for different HVDAC offsets was expected given the results from the mass spectrometer intercomparison mentioned above. The results from the measurements in Bremen show deviations in the opposite direction, as a consequence of the lower $^{46}\delta$ values measured on the MAT 253 mass spectrometer.

In consideration of our conclusions from the mass spectrometer intercomparison, we believe that the results given in rows 7 and 14 (Table 3) are our best and most accurate estimates for the absolute position-dependent isotope ratios of our reference gases.

Error estimation

In Table 4 we investigate the result for the combined MPI-1a and MPI-1b data set (row 7, Table 3) with respect to its sensitivity to the uncertainty of measured quantities and

Table 3 Overview of the final results for $^{1}\delta^{15}$N(MPI-1) and $^{2}\delta^{15}$N(MPI-2) deduced from the slopes of $^{31}\delta$ versus $^{46}\delta$ and $^{45}\delta$ versus $^{46}\delta$ in different mixing series[a]

Row	Mixing series	Analysis date	MS	HV off-set	$^{45}\delta$ versus $^{46}\delta$		$^{31}\delta$ versus $^{46}\delta$ MPI-1				
					Ordinate intercept (‰)	Slope	Ordinate intercept (‰)	Slope	$^{1}\delta^{15}$N (‰)	$^{2}\delta^{15}$N (‰)	Error
1	MPI-1a	June 2002	252 MPI	–38	0.01±0.01	0.00061±0.00000	–0.31±0.16	0.5068±0.0001	–18.33	20.35	0.26
2	Subset of MPI-1a	May 2003	252 MPI	–38	0.05±0.02	0.00049±0.00005	0.26±0.13	0.5072±0.0004	–17.07	19.09	0.96
3	Subset of MPI-1a	May 2003	252 MPI	–30	0.05±0.02	0.00049±0.00005	–0.01±0.10	0.5093±0.0003	–11.50	13.51	0.73
4	MPI-1b	May 2003	252 MPI	–38	0.01±0.00	0.00058±0.00002	0.06±0.09	0.5080±0.0004	–15.05	17.07	0.94
5	MPI-1b	May 2003	252 MPI	–30	0.01±0.00	0.00058±0.00002	0.03±0.04	0.5095±0.0002	–11.12	13.13	0.41
6	MPI-1a & MPI-1b	May 2003	252 MPI	–38	0.01±0.01	0.00057±0.00002	0.10±0.07	0.5077±0.0002	–15.85	17.87	0.62
7	MPI-1a & MPI-1b	May 2003	252 MPI	–30	0.01±0.01	0.00057±0.00002	0.02±0.04	0.5093±0.0001	–11.61	13.63	0.36
8	MPI-2a	June 2002	252 MPI	–38	0.00±0.00	0.00061±0.00000	0.84±0.19	0.5026±0.0001	–20.71	22.72	0.29
9	UCB-a	June 2002	252 UCB	–30	–0.01±0.03	0.00609±0.00014	–0.03±0.13	0.5161±0.0005	–12.55	14.57	1.41
10	UCB-b	May 2003	252 UCB	–30	–0.01±0.00	0.00509±0.00001	–0.04±0.06	0.5158±0.0003	–10.96	12.98	0.66
11	UCB-b	May 2003	253 Bremen	0	0.00±0.00	0.00507±0.00002	0.00±0.03	0.5172±0.0001	–7.16	9.18	0.35
12	UCB-b	May 2003	252 MPI	–38	0.00±0.01	0.00496±0.00003	0.01±0.09	0.5125±0.0004	–19.24	21.26	0.96
13	UCB-b	May 2003	252 MPI	–30	0.00±0.01	0.00496±0.00003	0.03±0.04	0.5144±0.0002	–14.14	16.16	0.44
14	UCB-a & UCB-b	June 2002 & May 2003	252 UCB	–30	0.02±0.06	0.00540±0.00026	–0.03±0.06	0.5159±0.0002	–11.43	13.45	0.62

[a]The error estimates are based on the $^{31}\delta$ versus $^{46}\delta$ slopes only. Measurements on the MAT 252 machines with an HV offset –30 are considered reliable, as explained in the text. Rows 6, 7, and 14 represent the combined data sets of rows 2 and 4, rows 3 and 7, and rows 9 and 10, respectively. Rows 7 and 14 represent our best estimate of the absolute position-dependent isotopic composition of gas MPI-1, based on the MPI and UCB mixing series

Table 4 Sensitivity of $^{1}\delta^{15}$N(MPI-1) and $^{2}\delta^{15}$N(MPI-2) to the uncertainties of measured quantities and absolute isotope ratios

Case	$^{45}R_{ref}$(MPI-1)	^{17}R(VSMOW)	$^{46}R_{ref}$(MPI-1)	$^{31}\delta$ verus $^{46}\delta$ slope	$^{45}\delta$ versus $^{46}\delta$ slope	s	$^{15}Z_1$	$^{15}Z_2$	$^{1}\delta^{15}$N (‰)	$^{2}\delta^{15}$N (‰)
Baseline	0.0077512	0.0003799	0.0020987	0.50943	0.00057	0.0822	0.00106	0.00106	–11.83[a]	13.85[a]
$^{31}\delta$ versus $^{46}\delta$ slope	0.0077512	0.0003799	0.0020987	±0.00014[a]	0.00057	0.0822	0.00106	0.00106	±0.36[a]	±0.36[a]
$^{45}\delta$ versus $^{46}\delta$ slope	0.0077512	0.0003799	0.0020987	0.50943	±0.00010[a]	0.0822	±0.00019[a]	±0.00019[a]	±0.25[a]	±0.25[a]
$^{15}Z_1/^{15}Z_2$ symmetry	0.0077512	0.0003799	0.0020987	0.50943	0.00057	0.0822	±0.00021[a]	±0.00021[a]	±0.24[a]	±0.24[a]
Scrambling	0.0077512	0.0003799	0.0020987	0.50943	0.00057	±0.005[a]	0.00106	0.00106	±0.15[a]	±0.15[a]
^{18}R(VSMOW)	0.0077512	0.0003799	±0.0000004[a]	0.50943	0.00057	0.0822	0.00106	0.00106	±0.30[a]	±0.30[a]
^{17}R(VSMOW)	0.0077512	±0.0000008[a]	0.0020987	0.50943	0.00057	0.0822	0.00106	0.00106	±0.26[a]	±0.26[a]
^{15}R(air–N_2)	±0.0000030[a]	0.0003799	0.0020987	0.50943	0.00057	0.0822	0.00106	0.00106	±0.49[a]	±0.49[a]
δ^{18}O(MPI-1) versus VSMOW	0.0077512	0.0003799	±0.0000004[a]	0.50943	0.00057	0.0822	0.00106	0.00106	±0.30[a]	±0.30[a]
δ^{15}N(MPI-1) versus air–N_2	±0.0000001[a]	0.0003799	0.0020987	0.50943	0.00057	0.0822	0.00106	0.00106	±0.07[a]	±0.01[a]
^{15}R(air–N_2) [18]	0.0077477[a]	0.0003799	0.0020987	0.50943	0.00057	0.0822	0.00106	0.00106	–0.56[a]	+0.56[a]
^{17}R(VSMOW) [28]	0.0077431[a]	0.0003720[a]	0.0020987	0.50943	0.00057	0.0822	0.00106	0.00106	–2.59[a]	+2.59[a]
^{17}R(VSMOW) [21]	0.0077561[a]	0.0003847[a]	0.0020987	0.50943	0.00057	0.0822	0.00106	0.00106	+1.57[a]	–1.57[a]

[a]These values show absolute differences to the baseline case (row 7 in Table 3), except for the values of ^{15}R(air–N_2), ^{17}R(VSMOW) and $^{45}R_{ref}$(MPI-1) in the last three rows where results from other absolute calibrations of these primary isotopic reference materials are given

the precision of the absolute isotope ratios of primary isotopic reference materials. The following uncertainties are considered: the standard deviations of the $^{31}\delta$ versus $^{46}\delta$ and $^{45}\delta$ versus $^{46}\delta$ slopes, variations of ±20% around an equal distribution between $^{14}N^{15}NO$ and $^{15}N^{14}NO$ ("$^{15}Z_1/^{15}Z_2$ symmetry") in the $^{15}N_2O$ sample, variations of ±0.5% for the scrambling coefficient s for a given mass spectrometer, the actual uncertainties of the absolute isotope ratios of air–N_2 and VSMOW, and the uncertainties of the "conventional" calibration of the nitrogen and oxygen isotope ratios of the MPI-1 reference gas relative to air–N_2 and VSMOW. The assumed uncertainty of the $^{15}Z_1/^{15}Z_2$ symmetry is most likely an overestimate. Rather, expectation of a symmetric distribution of ^{15}N between these two isotopomers seems reasonable, because the negligible abundance of $^{14}N_2O$ requires a nearly equal abundance of these isotopomers, since $^{15}N_2O$ has obviously the same ^{15}N abundance at both nitrogen positions. The actual uncertainty of the scrambling coefficient s is also much smaller (about 0.0001), but we wanted to show the variability in the resulting position-dependent δ values that would be observed if the scrambling coefficient was changing over longer timescales. The total uncertainty of the final $^{1}\delta^{15}$N and $^{2}\delta^{15}$N values can be estimated by the square root of the sum of squares of the individual uncertainties [34]. This gives a total uncertainty for the MPI-1 position-dependent calibration of ±0.9‰, and the isotopic composition of MPI-1 would then be $^{1}\delta^{15}$N=–11.6±0.9‰ and $^{2}\delta^{15}$N=13.6±0.9‰. However, we note that if there were systematic errors in the absolute isotope ratios used for the calculations, we would have arrived at different values. If, for example, the ^{17}R(VSMOW) value were actually 0.0003847, as measured recently by Assonov and Brenninkmeijer [21], then $^{1}\delta^{15}$N would be 1.6‰ higher and $^{2}\delta^{15}$N 1.6‰ lower (cf. last three rows of Table 4).

Intramolecular nitrogen isotope ratios of tropospheric N_2O

Kaiser et al. [17] recently reported high-precision measurements of tropospheric N_2O isotope ratios, which were measured versus the reference gas MPI-1. By using the new absolute calibration of the reference gas derived in this paper, we conclude that the position-dependent δ^{15}N values of tropospheric N_2O are $^{1}\delta^{15}$N(trop. N_2O)=–16.1±0.6‰ and $^{2}\delta^{15}$N(trop. N_2O)=29.5±0.6‰. The errors include only the standard deviation of the tropospheric measurements relative to the N_2O reference gas. A standard deviation of ±1.1‰ results if we include the uncertainty of the position-dependent calibration of the reference gas as described above. Another set of 75 tropospheric N_2O measurements was obtained between October 2001 and September 2002 at ground level on the UCB campus and gives similar results: $^{1}\delta^{15}$N(trop. N_2O)=–14.6±1.3‰ and $^{2}\delta^{15}$N(trop. N_2O)=27.2±1.3‰ (error includes tropospheric variability, measurement uncertainty, and the uncertainty of the position-dependent calibration). These values differ significantly from those of Yoshida and Toyoda [35] who found $^{1}\delta^{15}$N(trop. N_2O)=–2.4±1.6‰ and $^{2}\delta^{15}$N(trop. N_2O)=16.4±1.6‰.

The relative enrichment of ^{15}N at the central nitrogen over ^{15}N at the terminal nitrogen atom then is ($^{2}\delta^{15}$N–$^{1}\delta^{15}$N)/(1+$^{1}\delta^{15}$N)=46.3±1.4‰ [17] and 42.4±1.8‰ (UCB campus samples). These values are much larger than the estimate of 18.7±2.2‰ made by Yoshida and Toyoda [35]. We note that the expected variability of the tropospheric isotope ratios of N_2O is very low, so that this discrepancy must be explained by differences in the absolute isotope calibration of the respective reference gases. While the average ^{15}N composition of Yoshida and Toyoda's reference gas (–1.9‰ from the average of $^{1}\delta^{15}$N and $^{2}\delta^{15}$N or –2.2‰ from conversion with graphite) is sim-

ilar to our reference gases (+1.01 and 0.15‰ for MPI-1 and UCB-N_2O), the position-dependent enrichment is clearly distinct: Toyoda and Yoshida found for their reference gas $^1\delta^{15}N$=0.2±0.8‰ and $^1\delta^{15}N$=–4.0±0.4‰ [1]. However, the $\delta^{18}O$ value of their reference gas (23.3‰) also deviates substantially from ours (38.5‰ and 41.7‰ for MPI-1 and UCB-N_2O) and is closer to atmospheric oxygen (23.8‰) [36]. Commercial N_2O production usually starts from NH_4NO_3 [37], but some manufacturers also extract it from exhaust gas in adipic acid production (as in the case of our sample of MPI-2 obtained from Puritan-Bennet Medical Gases). Tracing back the original source of our the MPI-1 reference gas is difficult, because the supplier (Messer-Griesheim) only acts as a distributor of batches obtained on the world market. Most likely, though, the reference gas originates from Ijsfabriek Strombeek, Belgium, and is made by decomposition of NH_4NO_3. The nitrogen and oxygen isotopic composition of NH_4NO_3 is expected to be close to that of air because NH_3 is produced from air–N_2 in the Haber-Bosch process and HNO_3 is made by NH_3 oxidation with air (Ostwald process) [37]. However, isotopic fractionation may occur in later purification steps, which presumably proceed through distillation to obtain the high purity (grade 6.0 equivalent to 99.9999%) of the MPI-1 reference gas. Vapor pressures of isotopic N_2O species are known to increase in the order $^{14}N_2{}^{18}O$<$^{15}N^{14}N^{16}O$<$^{14}N^{15}N^{16}O$<$^{14}N_2{}^{16}O$ [38], which may explain the enrichment of $^{14}N^{15}N^{16}O$ over $^{15}N^{14}N^{16}O$ as well as the relative ^{18}O enrichment of the MPI-1 reference gas by 14.4‰ relative to air–O_2.

Conclusions

We have presented a new method to determine the absolute intramolecular (position-dependent) nitrogen isotope ratios of nitrous oxide by a purely mass spectrometric technique. The method can be rapidly implemented in any laboratory capable of doing intramolecular nitrogen isotope ratio measurements on N_2O and gives results of similar precision to the more laborious, wet-chemical technique of Toyoda and Yoshida [1]. The method is based on a series of mixtures of the unknown N_2O sample with different amounts of $^{15}N_2O$ and subsequent measurements of the $^{31}\delta$, $^{45}\delta$, and $^{46}\delta$ values. External amount of substance determinations are not required and would be much more difficult to achieve by conventional volumetric, manometric, or gravimetric techniques. Instead, the mass spectrometer itself is used as a tool of calibration, so that its high precision (about 10^{-5}) in relative isotope ratio measurements can be fully exploited. Accurate oxygen and average nitrogen isotope ratios of the unknown N_2O sample are needed for this method to work.

In order to obtain accurate results, the isotopic purity of the doubly labeled $^{15}N_2O$ sample must be established. $^{15}N^{14}N^{16}O$ and $^{14}N^{15}N^{16}O$ impurities can be accounted for by $^{45}\delta$ measurements. Measurements at *m*/*z* 12 allow for the correction of minor CO_2 impurities. The relative abundance of N in the N_2O mass spectrum must be measured to account for the production of ^{15}N ions from $^{15}N_2O$ since ^{15}N influences the measured ion current at *m*/*z* 30. Another important requirement for accurate results is an isotope ratio mass spectrometer that does not show any scale contraction. We have verified this for our instruments at the Mainz, Berkeley, and Bremen, as best as possible, using intercomparisons between different mass spectrometers, changes of the idle time between sample and reference measurement cycles, and measurements of sequences of N_2O samples enriched to very different degrees. From the evaluated results of this exercise, we have chosen those data sets that most likely represent the most accurate relative $^{31}\delta$, $^{45}\delta$, and $^{46}\delta$ measurements and have calculated the position-dependent nitrogen isotope composition of our reference gases. In conjunction with isotope ratio measurements of tropospheric N_2O measured in Mainz [17] and at UC Berkeley, we conclude that the $\delta^{15}N$ value of the terminal nitrogen atom in free tropospheric N_2O is $^1\delta^{15}N$=–16.2±1.1‰ and that of the central nitrogen atom is $^2\delta^{15}N$=29.6±1.1‰. Boundary layer air on the UC Berkeley campus gives similar results: $^1\delta^{15}N$=–14.6±1.3‰ and $^2\delta^{15}N$=27.2±1.3‰. The uncertainties include the long-term variability of tropospheric N_2O relative to the reference gas and the uncertainty of the reference gas calibration.

These values differ significantly from the results obtained by Yoshida and Toyoda [35], most probably due to differences in the reference gas calibration. A future direct reference gas intercomparison might be warranted, but will not resolve the differences in the position-dependent calibrations that were revealed by comparing the results for tropospheric N_2O. However, we note that the accuracy of our results depends on the accuracy of the absolute isotope ratios of the primary isotopic reference materials air–N_2 and VSMOW. If ^{15}R(air–N_2), ^{17}R(VSMOW), or ^{18}R(VSMOW) are wrong, our final results will necessarily be incorrect. For example, a recent recalibration has resulted in a higher ^{17}R(VSMOW) value [21] than measured previously [20], which would bring our results for tropospheric N_2O 1.6‰ closer to the results of Yoshida and Toyoda (Table 4). That said, one could also conclude that the absolute isotope ratios of the primary reference materials air–N_2 and VSMOW are not accurate (provided that Yoshida and Toyoda's relative calibration is correct). The "Institute for Reference Materials and Measurements" in Geel, Belgium, is currently pursuing efforts to recalibrate the absolute isotope ratios of VPDB–CO_2 [39], which is closely linked to VSMOW. This might lead to a change of ^{18}R(VSMOW) and therefore also to a change of the results from the present calibration.

Finally, we note that a similar technique to the one presented here for mixtures of the reference gas with doubly labeled $^{15}N_2O$ can be implemented by using $N^{15}NO$ or ^{15}NNO instead. It appears less elegant to us though, since one has to consider even more influences from impurities. The mathematical treatment and preliminary results from the application of these two related methods are given in the Appendices B and C.

Acknowledgements We would like to acknowledge Claus Koeppel and Tae Siek Rhee for help with the mass spectrometric measurements as well as Hairigh Avak and Jens Radke for assistance with the MAT 253 mass spectrometer in the Application Laboratory of Thermo Finnigan MAT, Bremen. Willi Brand is thanked for useful discussions on isotope ratio mass spectrometric finesses. John Crowley helped with the FTIR measurements. The work at UC Berkeley was supported by the US National Science Foundation Atmospheric Chemistry Program (ATM-9901463), the NASA Upper Atmospheric Research Program (NAG2–1483), the David and Lucile Packard Foundation, and the Earth Science Division, Lawrence Berkeley National Laboratory.

Appendix A: Keeling plots

The method of Sutka et al. [24] uses a so-called Keeling plot to determine the intramolecular nitrogen isotope distribution of their reference gas. This type of chart dates back to Charles D. Keeling [40] who used it to determine the unknown isotopic composition of CO_2 sources from atmospheric measurements of isotope and mixing ratios. The ordinate intercept in a plot of the isotope ratio (or δ value) versus the inverse of the mixing ratio gives the isotopic composition of the CO_2 source; the composition of atmospheric background CO_2 can be derived from the slope if the background mixing ratio is known. Transferring this approach to the calibration of their reference gas, Sutka and co-workers mixed different amounts of $^{14}N^{15}NO$ with their reference gas. One should bear in mind that for Sutka's application, the N_2O mixing ratio always equals 1, so that the "traditional" Keeling plot appears in an unconventional form at first sight. However, we will show how the "traditional" Keeling plot can be recovered from the form in which we make use of it here. The relative isotope enrichment of the mixture (δ_m) can be approximated by

$$Q_m\delta_m \approx Q_a\delta_a + Q_b\delta_b \tag{A1}$$

The indices "m", "a", and "b" represent the mixture, the $^{14}N^{15}NO$ sample (component A), and the reference gas (component B), respectively. Q_m is equal to Q_a+Q_b. Sutka and co-workers identify the quantity Q with the total number of N_2O molecules. However, to make expression A1 a mathematically accurate equation, Q has to be identified with the number of atoms of the light isotope (i.e., ^{14}N), indicated by a superscript "14":

$$^{14}Q_m\delta_m = {}^{14}Q_a\delta_a + {}^{14}Q_b\delta_b \tag{A2}$$

Approximating ^{14}Q by the total number of atoms leads to an error that increases with the isotope ratio. Although this error can be neglected for most other applications of Keeling plots, it is obviously desirable not to introduce unnecessary approximations in the calibration of a reference gas. We show in the following how this approximation can be avoided and also discuss why we believe that the slope of the Keeling plot shown in the paper by Sutka et al. [24] does not correspond to the expected slope.

To further simplify Eq. A2, the fractions of ^{14}N from components A and B are expressed relative to the total amount of ^{14}N, i.e.

$$^{14}x_a = {}^{14}Q_a / {}^{14}Q = {}^{14}Q_a / ({}^{14}Q_a + {}^{14}Q_b) \tag{A3}$$

$$^{14}x_b = {}^{14}Q_b / {}^{14}Q = 1 - {}^{14}x_a \tag{A4}$$

We then have

$$\delta = {}^{14}x_a\delta_a + {}^{14}x_b\delta_b = {}^{14}x_a\delta_a + (1 - {}^{14}x_a)\delta_b, \tag{A5}$$

which gives

$$\delta = {}^{14}x_a(\delta_a - \delta_b) + \delta_b. \tag{A6}$$

Equation A6 differs in two aspects from a "traditional" Keeling plot: firstly, $^{14}x_a$ would "traditionally" be expressed in terms of mixing ratios (μ) (i.e., $^{14}x_a = {}^{14}\mu_a / {}^{14}\mu$). However, for the present application, there are no components other than N_2O in the mixture, and $^{14}\mu$ is identical to 1. We note that $^{14}\mu_a$ in a "traditional" Keeling plot would be identified with the atmospheric background mixing ratio. Secondly, the approximation $^{14}\mu \approx \mu$ or $^{14}x_a \approx x_a$ is often made, but this is only valid for small enrichments, not for highly enriched compounds. Continuing with the non-approximated Eq. A6, we calculate the molar fraction of component A (x_a) from $^{14}x_a$:

$$x_a = \frac{{}^{14}Q_a + {}^{15}Q_a}{{}^{14}Q_a + {}^{15}Q_a + {}^{14}Q_b + {}^{15}Q_b} = \frac{{}^{14}x_a(1+R_a)}{{}^{14}x_a(R_a - R_b) + 1 + R_b} \tag{A7}$$

where R stands for the isotope ratio. Solving for $^{14}x_{gives}$:

$$^{14}x_a = \frac{x_a(1+R_b)}{1 + R_a - x_a(R_a - R_b)} \tag{A8}$$

We then have for δ:

$$\delta = (\delta_a - \delta_b)\frac{(1+R_b)x_a}{1 + R_a - x_a(R_a - R_b)} + \delta_b. \tag{A9}$$

Therefore, a "Keeling plot" of δ versus x_a (or versus $1/\mu$ for the "traditional" Keeling plot) is actually not a straight line, but a hyperbola. It can be expanded to a Taylor series in terms of x_a around x_a=0:

$$\delta = (\delta_a - \delta_b)\frac{1+R_b}{1+R_a}\left(x_a + \frac{x_a^2}{2} + \frac{x_a^3(R_a - R_b)}{3(1+R_a)} + O(x_a^4)\right) + \delta_b \tag{A10}$$

In other words, one should really fit a polynomial to a "Keeling plot" of δ versus x_a, not a line, at least for large values of x_a. The value of x_a does not exceed 0.001 for the data set of Sutka et al. [24], so that we can obtain the expected slope m from the linear term in Eq. A10:

$$m = (\delta_a - \delta_b)\frac{1+R_b}{1+R_a} \tag{A11}$$

R_b and R_a can also be expressed in terms of δ values (with R_{ref} being the isotope ratio of the primary reference material, i.e., air–N_2):

$$m = (\delta_a - \delta_b)\frac{1 + R_{ref}(1+\delta_b)}{1 + R_{ref}(1+\delta_a)} \tag{A12}$$

From Fig. 2 in Sutka et al. [24], we get δ_b=0.00361 and m=138.52. With R_{ref}=0.0036782 [18], we calculate δ_a=281.3

or 281.3×10³‰. This corresponds to an isotope ratio R_a of 1.038, or almost equal amounts of ^{15}N and ^{14}N. However, the expected ratio would be 49 if the $^{14}N^{15}NO$ sample of Sutka and co-workers were really 98% $^{14}N^{15}N^{16}O$ as stated and if the remaining 2% were $^{14}N_2{}^{16}O$. The ratio would be even larger if the abundance of $^{14}N_2{}^{16}O$ were less than 2%.

Conversely, if one assumes R_a to be 49, then m equals 267.5, or roughly double the slope stated by Sutka et al. [24]. We conclude that there must be an error in their data reduction procedure. Furthermore, we note that if there were $^{15}N_2{}^{16}O$ or $^{15}N^{14}N^{16}O$ present in the $N^{15}NO$ sample, one would obtain an ordinate intercept that does not correspond to the true δ value of the reference gas. Finally, the scatter around the linear fit is large, most likely due to the volumetric method to prepare the mixtures of reference gas and $N^{15}NO$. This difficulty can be avoided if simultaneous $^{45}\delta$ measurements are used, similar to the approach we present as the main subject of this paper. The detailed theoretical treatment required for this alternative to the approach of Sutka et al. [24] is given in Appendix B. The same approach can also be used with ^{15}NNO, and the theoretical treatment for that is slightly different and is given in Appendix C. In both these appendices, we also show preliminary results demonstrating that we can derive position-dependent isotopic compositions from mixing series of ^{15}NNO or $N^{15}NO$ with the MPI-1 reference gas. These mixing series were initially intended to determine the scrambling coefficient s. The results are preliminary in that the mixing series consist of only three samples (and therefore four measurements) and were measured on a Micromass Prism II mass spectrometer, which was not included in our mass spectrometer intercomparison (see Section "Intercomparison of $^{45}\delta$, $^{46}\delta$, and $^{31}\delta$ values" above). Nevertheless, the values obtained are similar to those obtained for the series consisting of diluting doubly labeled N_2O and demonstrate that these other approaches, when combined with the correct mathematical treatment, should give similar results.

Appendix B: absolute position-dependent calibration with $N^{15}NO$

$N^{15}NO$ can be used in a similar way as $^{15}N_2O$ to calibrate the position-dependent isotope ratios of a given N_2O reference gas. Starting from the set of equations for the "molecular isotope ratios" of the reference gas

$$^{45}R_{\mathrm{ref}} = {}^{15}R_{1,\mathrm{ref}} + {}^{15}R_{2,\mathrm{ref}} + {}^{17}R_{\mathrm{ref}} \tag{B1}$$

$$^{46}R_{\mathrm{ref}} = \left({}^{15}R_{1,\mathrm{ref}} + {}^{15}R_{2,\mathrm{ref}}\right){}^{17}R_{\mathrm{ref}} + {}^{18}R_{\mathrm{ref}} + {}^{15}R_{1,\mathrm{ref}} + {}^{15}R_{2,\mathrm{ref}} \tag{B2}$$

$$^{31}R_{\mathrm{s,ref}} = \frac{s\,{}^{15}R_{1,\mathrm{ref}} + (1-s)\,{}^{15}R_{2,\mathrm{ref}} + {}^{15}R_{1,\mathrm{ref}}\,{}^{15}R_{2,\mathrm{ref}} + {}^{17}R_{\mathrm{ref}}\left[1 + s\,{}^{15}R_{2,\mathrm{st}} + (1-s)\,{}^{15}R_{1,\mathrm{st}}\right]}{1 + s\,{}^{15}R_{2,\mathrm{ref}} + (1-s)\,{}^{15}R_{1,\mathrm{ref}}} \tag{B3}$$

we then arrive at the following equations for the $N^{15}NO$-amended reference gas:

$$^{45}R = \frac{{}^{15}R_{1,\mathrm{ref}} + {}^{15}R_{2,\mathrm{ref}} + {}^{17}R_{\mathrm{ref}} + {}^{456}R\left(1 + {}^{15}Y_1 + {}^{14}Y_0\,{}^{17}Y\right)}{1 + {}^{456}R\,{}^{14}Y_0} \tag{B4}$$

$$^{45}R = \frac{\left({}^{15}R_{1,\mathrm{ref}} + {}^{15}R_{2,\mathrm{ref}}\right){}^{17}R_{\mathrm{ref}} + {}^{18}R_{\mathrm{ref}} + {}^{15}R_{1,\mathrm{ref}}\,{}^{15}R_{2,\mathrm{ref}} + {}^{456}R\left[{}^{18}Y\,{}^{14}Y_0 + {}^{15}Y_{1+2} + {}^{17}Y\left(1 + {}^{15}Y_1\right)\right]}{1 + {}^{456}R\,{}^{14}Y_0} \tag{B5}$$

$$^{31}R_{\mathrm{s,ref}} = \frac{\begin{array}{c} s\,{}^{15}R_{1,\mathrm{ref}} + (1-s)\,{}^{15}R_{2,\mathrm{ref}} + {}^{15}R_{1,\mathrm{ref}}\,{}^{15}R_{2,\mathrm{ref}} \\ + {}^{17}R_{\mathrm{ref}}\left[1 + s\,{}^{15}R_{2,\mathrm{ref}} + (1-s)\,{}^{15}R_{1,\mathrm{ref}}\right] \end{array}}{1 + s\,{}^{15}R_{2,\mathrm{ref}} + (1-s)\,{}^{15}R_{1,\mathrm{ref}} + p\,{}^{15}R_{1,\mathrm{ref}}\,{}^{15}R_{2,\mathrm{ref}}} + \frac{\begin{array}{c} {}^{456}R\left[{}^{14}Y_0 + s + (1-s)\,{}^{15}Y_1 + p\,{}^{15}Y_{1+2}\right] \\ {}^{456}R\left\{\begin{array}{l} s\,{}^{15}Y_1 + 1 - s + {}^{15}Y_{1+2} \\ + {}^{17}Y\left[{}^{14}Y_0 + s + (1-s)\,{}^{15}Y_1\right] \end{array}\right\} \end{array}}{1 + s\,{}^{15}R_{2,\mathrm{ref}} + (1-s)\,{}^{15}R_{1,\mathrm{ref}} + p\,{}^{15}R_{1,\mathrm{ref}}\,{}^{15}R_{2,\mathrm{ref}} + {}^{456}R\left[{}^{14}Y_0 + s + (1-s)\,{}^{15}Y_1 + p\,{}^{15}Y_{1+2}\right]} \tag{B6}$$

The added $^{14}N^{15}N^{16}O$ is represented by the term ^{456}R. ^{456}R equals $N_C(^{14}N^{15}N^{16}O)/N_{\mathrm{ref}}(^{14}N_2{}^{16}O)$. The abundance of $^{14}N_2{}^{16}O$, $^{15}N^{14}N^{16}O$, $^{15}N_2{}^{16}O$, $^{14}N^{15}N^{17}O$, $^{15}N^{14}N^{17}O$, and $^{14}N_2{}^{18}O$ in the $N^{15}NO$ sample are taken into account by the following terms: $^{14}Y_0$ is $N_C(^{14}N_2{}^{16}O)/N_C(^{14}N^{15}N^{16}O)$, $^{15}Y_1$ is $N_C(^{15}N^{14}N^{16}O)/N_C(^{14}N^{15}N^{16}O)$, $^{15}Y_{1+2}$ is $N_C(^{15}N_2{}^{16}O)/N_C(^{14}N^{15}N^{16}O)$, ^{17}Y is $N_C(^{14}N^{15}N^{17}O)/N_C(^{14}N^{15}N^{16}O)$, and ^{18}Y is $N_C(^{14}N^{15}N^{18}O)/N_C(^{14}N^{15}N^{16}O)$, in which N_C and N_{ref} are the number of molecules from labeled N_2O ($^{14}N^{15}N^{16}O$) and the reference gas, respectively. A statistical oxygen isotope distribution for $N^{15}NO$ is assumed. The contribution of ^{15}N formation from $^{15}N_2{}^{16}O$ to the m/z 30 ion current is represented by the terms $p\,{}^{15}R_{1,\mathrm{ref}}\,{}^{15}R_{2,\mathrm{ref}}$ and $p\,{}^{15}Y_{1+2}$. Then, the following relationships for the δ values hold:

$$^{45}\delta = \frac{{}^{456}R}{{}^{45}R_{\mathrm{ref}}}\,\frac{1 + {}^{15}Y_1 + {}^{14}Y_0\,{}^{17}Y - {}^{14}Y_0\,{}^{45}R_{\mathrm{ref}}}{1 + {}^{456}R\,{}^{14}Y_0} \tag{B7}$$

$$^{46}\delta = \frac{{}^{456}R}{{}^{46}R_{\mathrm{ref}}}\,\frac{{}^{18}Y\,{}^{14}Y_0 + {}^{15}Y_{1+2} + {}^{17}Y\left(1 + {}^{15}Y_1\right) - {}^{14}Y_0\,{}^{46}R_{\mathrm{ref}}}{1 + {}^{456}R\,{}^{14}Y_0} \tag{B8}$$

$$^{31}\delta = \frac{{}^{456}R}{{}^{31}R_{\mathrm{s,ref}}}\,\frac{\begin{array}{c} s\,{}^{15}Y_1 + 1 - s + {}^{15}Y_{1+2} + {}^{17}Y\left[{}^{14}Y_0 + s + (1-s)\,{}^{15}Y_1\right] \\ - {}^{31}R_{\mathrm{s,ref}}\left[{}^{14}Y_0 + s + (1-s)\,{}^{15}Y_1 + p\,{}^{15}Y_{1+2}\right] \end{array}}{\begin{array}{l} 1 + s\,{}^{15}R_{2,\mathrm{ref}} + (1-s)\,{}^{15}R_{1,\mathrm{ref}} + p\,{}^{15}R_{1,\mathrm{ref}}\,{}^{15}R_{2,\mathrm{ref}} \\ \quad + {}^{456}R\left[{}^{14}Y_0 + s + (1-s)\,{}^{15}Y_1 + p\,{}^{15}Y_{1+2}\right] \end{array}} \tag{B9}$$

We have re-evaluated our own old measurements of the scrambling coefficient on a Micromass Prism II mass spectrometer and obtained the following final results for a sample of the MPI-1 reference gas: $^1\delta^{15}N$=–23.6±0.7‰ and $^2\delta^{15}N$=25.6±0.7‰. The uncertainties only consider the standard deviation of the $^{31}\delta$ versus $^{46}\delta$ slope. $^{14}Y_0$ was 0.00613, ^{18}Y was 0.00210, and $^{15}Y_{1+2}$+^{17}Y was 0.00478. Given the ^{18}Y value, we have assumed a normal ^{17}O abundance, so that ^{17}Y was 0.00039 and $^{15}Y_{1+2}$ equaled 0.00439. We have assumed an abundance of about 0.001 for the undesired isotopomer, so that $^{15}Y_1$ is 0.001. These results should be considered very preliminary inasmuch as the $^1\delta^{15}N$ and $^2\delta^{15}N$ are concerned since only four $^{31}\delta$ measurements were available. In general, this seems to be a viable approach and the results are in the general range of what was

found with a series of mixtures of $^{15}N_2O$ with N_2O reference gases.

Appendix C: absolute position-dependent calibration with ^{15}NNO

^{15}NNO can be used in a similar way as $^{15}N_2O$ to calibrate the position-dependent isotope ratios of a given N_2O reference gas and is very similar to the approach for N^{15}NO detailed in Appendix B. Starting from the set of equations for the "molecular isotope ratios" of the reference gas

$$^{45}R_{\mathrm{ref}} = {}^{15}R_{1,\mathrm{ref}} + {}^{15}R_{2,\mathrm{ref}} + {}^{17}R_{\mathrm{ref}} \tag{C1}$$

$$^{46}R_{\mathrm{ref}} = \left({}^{15}R_{1,\mathrm{ref}} + {}^{15}R_{2,\mathrm{ref}}\right){}^{17}R_{\mathrm{ref}} + {}^{18}R_{\mathrm{ref}} + {}^{15}R_{1,\mathrm{ref}}\,{}^{15}R_{2,\mathrm{ref}} \tag{C2}$$

$$^{31}R_{\mathrm{s,ref}} = \frac{\begin{array}{c} s\,{}^{15}R_{1,\mathrm{ref}} + (1-s)\,{}^{15}R_{2,\mathrm{ref}} + {}^{15}R_{1,\mathrm{ref}}\,{}^{15}R_{2,\mathrm{ref}} \\ + {}^{17}R_{\mathrm{ref}}\left[1 + s\,{}^{15}R_{2,\mathrm{st}} + (1-s)\,{}^{15}R_{1,\mathrm{st}}\right] \end{array}}{1 + s\,{}^{15}R_{2,\mathrm{ref}} + (1-s)\,{}^{15}R_{1,\mathrm{ref}}} \tag{C3}$$

we then arrive at the following equations for the ^{15}NNO-amended reference gas:

$$^{45}R = \frac{{}^{15}R_{1,\mathrm{ref}} + {}^{15}R_{2,\mathrm{ref}} + {}^{17}R_{\mathrm{st}} + {}^{546}R\left(1 + {}^{15}X_2 + {}^{14}X_0\,{}^{17}X\right)}{1 + {}^{546}R\,{}^{14}X_0} \tag{C4}$$

$$^{46}R = \frac{\begin{array}{c} \left({}^{15}R_{1,\mathrm{ref}} + {}^{15}R_{2,\mathrm{ref}}\right){}^{17}R_{\mathrm{ref}} + {}^{18}R_{\mathrm{ref}} + {}^{15}R_{1,\mathrm{ref}}\,{}^{15}R_{2,\mathrm{ref}} \\ + {}^{546}R\left[{}^{18}X\,{}^{14}X_0 + {}^{15}X_{1+2} + {}^{17}X\left(1 + {}^{15}X_2\right)\right] \end{array}}{1 + {}^{546}R\,{}^{14}X_0} \tag{C5}$$

$$^{31}R_{\mathrm{s,ref}} = \frac{\begin{array}{c} s\,{}^{15}R_{1,\mathrm{ref}} + (1-s)\,{}^{15}R_{2,\mathrm{ref}} + {}^{15}R_{1,\mathrm{ref}}\,{}^{15}R_{2,\mathrm{ref}} \\ + {}^{17}R_{\mathrm{ref}}\left[1 + s\,{}^{15}R_{2,\mathrm{ref}} + (1-s)\,{}^{15}R_{1,\mathrm{ref}}\right] \end{array}}{\begin{array}{c} 1 + s\,{}^{15}R_{2,\mathrm{ref}} + (1-s)\,{}^{15}R_{1,\mathrm{ref}} + p\,{}^{15}R_{1,\mathrm{ref}}\,{}^{15}R_{2,\mathrm{ref}} \\ + {}^{546}R\left[{}^{14}X_0 + s\,{}^{15}X_2 + 1 - s + p\,{}^{15}X_{1+2}\right] \end{array}} + \frac{{}^{546}R\left\{\begin{array}{c} s\,{}^{15}X_1 + 1 - s + {}^{15}X_{1+2} \\ + {}^{17}X\left[{}^{14}X_0 + s\,{}^{15}X_2 + 1 - s\right] \end{array}\right\}}{\begin{array}{c} 1 + s\,{}^{15}R_{2,\mathrm{ref}} + (1-s)\,{}^{15}R_{1,\mathrm{ref}} + p\,{}^{15}R_{1,\mathrm{ref}}\,{}^{15}R_{2,\mathrm{ref}} \\ + {}^{546}R\left[{}^{14}X_0 + s\,{}^{15}X_2 + 1 - s + p\,{}^{15}X_{1+2}\right] \end{array}} \tag{C6}$$

The added $^{15}NN^{16}O$ is represented by the term ^{546}R. ^{546}R equals $N_C(^{15}N^{14}N^{16}O)/N_{\mathrm{ref}}(^{14}N_2{}^{16}O)$. The abundance of $^{14}N_2{}^{16}O$, $^{15}N_2{}^{16}O$, $^{14}N^{15}N^{17}O$, $^{15}N^{14}N^{17}O$, and $^{14}N_2{}^{18}O$ in the ^{15}NNO sample are taken into account by the following terms: $^{14}X_0$ is $N_C(^{14}N_2{}^{16}O)/N_C(^{15}N^{14}N^{16}O)$, $^{15}X_2$ is $N_C(^{14}N^{15}N^{16}O)/N_C(^{15}N^{14}N^{16}O)$, $^{15}X_{1+2}$ is $N_C(^{15}N_2{}^{16}O)/N_C(^{15}N^{14}N^{16}O)$, ^{17}X is $N_C(^{15}N^{14}N^{17}O)/N_C(^{15}N^{14}N^{16}O)$, and ^{18}X is $N_C(^{15}N^{14}N^{18}O)/N_C(^{15}N^{14}N^{16}O)$, where N_C and N_{ref} are the number of molecules from labeled N_2O ($^{15}N^{14}N^{16}O$) and the reference gas, respectively. A statistical oxygen isotope distribution is assumed. The contribution of ^{15}N formation from $^{15}N_2{}^{16}O$ to the m/z 30 ion current is represented by the terms $p\,{}^{15}R_{1,\mathrm{ref}}\,{}^{15}R_{2,\mathrm{ref}}$ and $p\,{}^{15}X_{1+2}$. Then, the following relationships for the δ values hold:

$$^{45}\delta = \frac{^{546}R}{^{45}R_{\mathrm{ref}}}\,\frac{1 + {}^{15}X_2 + {}^{14}X_0\,{}^{17}X - {}^{14}X_0\,{}^{45}R_{\mathrm{ref}}}{1 + {}^{546}R\,{}^{14}X} \tag{C7}$$

$$^{46}\delta = \frac{^{546}R}{^{46}R_{\mathrm{ref}}}\,\frac{{}^{18}X\,{}^{14}X_0 + {}^{15}X_{1+2} + {}^{17}X\left(1 + {}^{15}X_2\right) - {}^{14}X_0\,{}^{46}R_{\mathrm{ref}}}{1 + {}^{546}R\,{}^{14}X_0} \tag{C8}$$

$$^{31}\delta = \frac{^{546}R}{^{31}R_{\mathrm{s,ref}}}\,\frac{\begin{array}{c} s + (1-s)\,{}^{15}X_2 + {}^{15}X_{1+2} + {}^{17}X\left[{}^{14}X_0 + s\,{}^{15}X_2 + 1 - s\right] \\ - {}^{31}R_{\mathrm{s,ref}}\left[{}^{14}X_0 + s\,{}^{15}X_2 + 1 - s + p\,{}^{15}X_{1+2}\right] \end{array}}{\begin{array}{c} 1 + s\,{}^{15}R_{2,\mathrm{ref}} + (1-s)\,{}^{15}R_{1,\mathrm{ref}} + p\,{}^{15}R_{1,\mathrm{ref}}\,{}^{15}R_{2,\mathrm{ref}} \\ + {}^{546}R\left[{}^{14}X_0 + s\,{}^{15}X_2 + 1 - s + p\,{}^{15}X_{1+2}\right] \end{array}} \tag{C9}$$

We have re-evaluated our own old measurements of the scrambling coefficient on a Micromass Prism II mass spectrometer and obtained the following final results for a sample of the MPI-1 reference gas: $^1\delta^{15}$N=–18±7‰ and $^2\delta^{15}$N=21±7‰. The uncertainties only consider the standard deviation of the $^{31}\delta$ versus $^{46}\delta$ slope. $^{14}X_0$ was 0.00380, ^{18}X was 0.00210, and $^{15}X_{1+2}$+^{17}X was 0.00430. Given the ^{18}X value, we have assumed a normal ^{17}O abundance, so that ^{17}X was 0.00039 and $^{15}X_{1+2}$ equaled 0.00391. We have assumed an abundance of about 0.001 for the undesired isotopomer, so that $^{15}X_2$ is 0.001. These results should be considered very preliminary inasmuch as the $^1\delta^{15}$N and $^2\delta^{15}$N are concerned since only four $^{31}\delta$ measurements were available. Therefore, the relatively large uncertainty of the position-dependent δ^{15}N is possibly not meaningful, and we would actually expect a smaller true uncertainty, given the analytical precision of the mass spectrometer. In any case, the results seem to be in the range of what was found with $^{15}N_2O$.

Appendix D: purity of the $^{15}N_2O$ samples

The $^{45}\delta$ versus $^{46}\delta$ slopes differ by about a factor of 10 for mixtures of the reference gases with MPI-$^{15}N_2O$ and UCB-$^{15}N_2O$. This is due to the presence of a larger fraction of $^{14}N^{15}N^{16}O$ and $^{15}N^{14}N^{16}O$ in the UCB-$^{15}N_2O$ sample. MPI-$^{15}N_2O$ was purchased in 1999 from ICON Isotopes, Summit, NJ, USA, whereas UCB-$^{15}N_2O$ was acquired more than 25 years ago from Prochem, British Oxygen Co. The isotopic purity of the $^{15}N_2O$ affects the $^{31}\delta$ measurement, but not the $^{46}\delta$ measurement, and thus leads to a change of the slope $\partial^{31}\delta/\partial^{46}\delta$. We have taken this difference into account as explained in the theoretical section of this paper.

Another complication can arise from the presence of $^{14}N_2{}^{16}O$ in the $^{15}N_2O$-sample. Therefore, ion currents at m/z 44, 45, 46, 47, and 48 for "pure MPI-$^{15}N_2O$" were determined and normalized to the total ion current of these masses. Contributions of 0.02%, 0.21%, 99.52%, 0.04‰, and 0.21 %, respectively could be identified. These values document the high purity of the $^{15}N_2O$ sample, but also show the presence of a small isotopic contamination at m/z 45. The proportions of mass 47 and 48 indicate a normal oxygen isotope composition for $^{15}N_2O$. Measurement of the $^{12}C^+$ fragment shows that the minor signal at m/z 44 was caused exclusively by a small amount of CO_2. Thus, $^{13}C^{16}O_2$ should make only a very minor contribution (given its natural abundance relative to $^{12}C^{16}O_2$), and the signal at m/z 45 must therefore be caused by $^{15}N^{14}N^{16}O$ and $^{14}N^{15}N^{16}O$.

Similarly, we conclude that there is no significant $^{14}N_2{}^{16}O$ impurity present in the MPI-$^{15}N_2O$ sample.

The ratio of $^{15}N^{14}N^{16}O+^{14}N^{15}N^{16}O$ impurity to the desired isotopologue $(^{15}N_2{}^{16}O)$, $^{15}Z_1 + {}^{15}Z_2 = [x(^{14}N^{15}N^{16}O) + x(^{15}N^{14}N^{16}O)]/x(^{15}N_2{}^{16}O)$, is calculated to be 0.00216. However, this value may be slightly influenced by mass discrimination effects in the inlet or ion source. An independent estimate of $^{15}Z_1+^{15}Z_2$ can be derived from the $^{45}\delta$ versus $^{46}\delta$ slopes using Eq. 17. $^{45}R_{\mathrm{ref}}/^{46}R_{\mathrm{ref}}$ is known from the calibration of the N_2O reference gas [17] and can be inferred for MPI-2 from its δ values measured against the N_2O reference gas (Table 2). $^{15}Z_1+^{15}Z_2=0.00223\pm0.00001$ is derived from MPI-1 from the slopes in Fig. 1a and rows 1 and 8 in Table 3, in agreement with the ratio of 0.00223± 0.00001 derived from MPI-2. However, we note that measurements at different times gave slightly different slopes for unknown reasons. The variations of the slope have been included in the estimated total uncertainty of the absolute intramolecular nitrogen isotope ratios.

References

1. Toyoda S, Yoshida N (1999) Anal Chem 71:4711–4718
2. Brenninkmeijer CAM, Röckmann T (1999) Rapid Commun Mass Spectrom 13:2028–2033
3. Esler MB, Griffith DWT, Turatti F, Wilson SR, Rahn T, Zhang H (2000) Chemosphere Global Change Sci 2:445–454
4. Uehara K, Yamamoto K, Kikugawa T, Yoshida N (2001) Sens Actuators B 74:173–178
5. Kaiser J, Röckmann T, Brenninkmeijer CAM (2002) Phys Chem Chem Phys 4:4220–4230. DOI 10.1039/B204837J
6. Kaiser J, Röckmann T, Brenninkmeijer CAM, Crutzen PJ (2003) Atmos Chem Phys 3:303–313
7. Kaiser J, Brenninkmeijer CAM, Röckmann T (2002) J Geophys Res 107:4214. DOI10.1029/2001JD001506
8. Röckmann T, Kaiser J, Brenninkmeijer CAM, Crowley JN, Borchers R, Brand WA, Crutzen PJ (2001) J Geophys Res 106: 10403–10410
9. Toyoda S, Yoshida N, Urabe T, Aoki S, Nakazawa T, Sugawara S, Honda H (2001) J Geophys Res 106:7515–7522
10. Griffith DWT, Toon GC, Sen B, Blavier J-F, Toth RA (2000) Geophys Res Lett 27:2485–2488
11. Pérez T, Trumbore SE, Tyler SC, Matson PA, Ortiz-Monasterio I, Rahn T, Griffith DWT (2001) J Geophys Res 106:9869–9878
12. Yamulki S, Toyoda S, Yoshida N, Veldkamp E, Grant B, Bol R (2001) Rapid Commun Mass Spectrom 15:1263–1269
13. Popp BN, Westley MB, Toyoda S, Miwa T, Dore JE, Yoshida N, Rust TM, Sansone FJ, Russ ME, Ostrom NE, Ostrom PH (2002) Global Biogeochem Cycles 16:1064. DOI 10.1029/2001GB001806
14. Toyoda S, Yoshida N, Miwa T, Matsui Y, Yamagishi H, Tsunogai U, Nojiri Y, Tsurushima N (2002) Geophys Res Lett 29:10.1029/2001GL014311
15. Stein LY, Yung YL (2003) Annu Rev Earth Planet Sci 31: 329–356. DOI 10.1146/annurev.earth.31.110502.080901
16. Friedman L, Bigeleisen J (1950) J Chem Phys 18:1325–1331
17. Kaiser J, Röckmann T, Brenninkmeijer CAM (2003) J Geophys Res 108:4476 DOI 10.1029/2003JD003613
18. Junk G, Svec HJ (1958) Geochim Cosmochim Acta 14:234–243
19. Baertschi P (1976) Earth Planet Sci Lett 31:341–344
20. Li W-J, Ni B, Jin D, Chang T-L (1988) Chin Sci Bull 33: 1610–1613
21. Assonov SS, Brenninkmeijer CAM (2003) Rapid Commun Mass Spectrom 17:1017–1029
22. De Bièvre P, Valkiers S, Peiser HS, Taylor PDP, Hansen P (1996) Metrologia 33:447–455
23. Bigeleisen J, Friedman L (1950) J Chem Phys 18:1656–1659
24. Sutka RL, Ostrom NE, Ostrom PH, Gandhi H, Breznak JA (2003) Rapid Commun Mass Spectrom 17:738–745
25. Brenna JT, Corso TN, Tobias HJ, Caimi RJ (1997) Mass Spectrom Rev 16:227–258
26. Coplen TB (1994) Pure Appl Chem 66:273–276
27. Trolier M, White JWC, Tans PP, Masarie KA, Gemery PA (1996) J Geophys Res 101:25897–25916
28. Craig H (1957) Geochim Cosmochim Acta 12:133–149
29. Gonfiantini R, Stichler W, Rozanski K (1995) In: Reference and intercomparison materials for stable isotopes of light elements. International Atomic Energy Agency, Vienna, pp 13–29
30. Garber EAE, Hollocher TC (1982) J Biol Chem 257:4705–4708
31. Begun GM, Landau L (1961) J Chem Phys 35:547–551
32. Meijer HAJ, Neubert REM, Visser GH (2000) Int J Mass Spectrom 198:45–61
33. Kaiser J (2002) Stable isotope investigations of atmospheric nitrous oxide. Johannes Gutenberg-Universität, Mainz http://archivmed.uni.mainz.de/pub/2003/0004/diss.pdf
34. Hund E, Massart DL, Smeyers-Verbeke J (2001) Trends Anal Chem 20:394–406
35. Yoshida N, Toyoda S (2000) Nature 405:330–334
36. Coplen TB, Hopple JA, Böhlke JK, Peiser HS, Rieder SE, Krouse HR, Rosman KJR, Ding T, Vocke J, R. D., Révész KM, Lamberty A, Taylor P, De Bièvre P (2002) Compilation of minimum and maximum isotope ratios of selected elements in naturally occurring materials and reagents. US Geological Survey Water-Resources Investigations Report 01–4222, p 41
37. Thiemann M, Scheibler E, Wiegand KW (1991) In: Elvers B, Hawkins S, Schulz G (eds) Ullmann's encyclopedia of industrial chemistry, Vol A17. VCH Verlagsgesllschaft, Weinheim, pp 293–339
38. Jancso G, van Hook WA (1974) Chem Rev 74:689–750
39. Nørgaard JV, Valkiers S, Van Nevel L, Vendelbo E, Papadakis I, Bréas O, Taylor PDP (2002) Anal Bioanal Chem 374: 1147–1154
40. Keeling CD (1958) Geochim Cosmochim Acta 13:322–334
41. Chang T-L, Li W-J (1990) Chin Sci Bull 35:290–296
42. Coplen TB, Krouse HR, Böhlke JK (1992) Pure Appl Chem 64:907–908